Spatial expression of an mRNA encoding Tie2-agonist in the capillary endothelium of the lung prevents pulmonary vascular leakage

Katrin Radloff[1,*], Birgitt Gutbier[2,*], Charlotte Maeve Dunne[3,4], Hanieh Moradian[3,4], Marko Schwestka[3,4], Manfred Gossen[3,4], Katharina Ahrens[2], Laura Kneller[2], Yadong Wang[2], Akanksha Moga[1], Leonidas Gkionis[1], Oliver Keil[1], Volker Fehring[1], Daniel Tondera[1], Klaus Giese[1], Ansgar Santel[1], Jörg Kaufmann[1,#], and Martin Witzenrath[2,#]

[1] Pantherna Therapeutics GmbH, 16761 Hennigsdorf, Germany

[2] Department of Infectious Diseases and Respiratory Medicine, Charité-Universitätsmedizin Berlin, corporate member of Freie Universität Berlin and Humboldt-Universität zu Berlin, 10117, Berlin, Germany

[3] Institute of Active Polymers, Helmholtz-Zentrum Hereon, 14513 Teltow, Germany

[4] Berlin-Brandenburg Center for Regenerative Therapies (BCRT) Charité Campus Virchow Klinikum, 13353 Berlin, Germany

[*] Authors contributed equally to this work

[#] Corresponding authors

Abstract

Angiopoietin ligands Ang1 and Ang2 and the Tie2 receptor tyrosine kinases form an endothelial signaling pathway regulating vascular homeostasis and controlling vessel permeability, inflammation and angiogenic responses. Whereas Ang1-mediated Tie2 activation reduces inflammation and endothelial permeability, its antagonist, Ang2 increases it. Increased plasma Ang2 levels are associated with poor outcomes in patients with acute lung injury (ALI), as well as in acute respiratory distress syndrome (ARDS).

In the study presented here we tested the effect of a novel synthetic, nucleoside-modified mRNA-76 encoding for a hyperactive Ang1 derived fusion protein (COMP-Ang1) on attenuating post-inflammation vascular leakage. COMP-Ang1 mRNA was formulated into a cationic lipid nanoparticle (cLNP) using an optimized mixture of three different lipids and a microfluidic mixing technology. After intravenous injection, the respective mRNA-loaded LNPs were found to be delivered predominantly to the endothelial cells of the lung, while sparing other vascular beds. Also, the specific multimeric folding of the COMP-Ang1 protein complex appeared to be pivotal for its activity in preventing vascular leakage and in restoring the alveolar-endothelial barrier function in the inflamed and injured pulmonary vasculature. The mode of action of mRNA-76, such as its activation of the Tie2 signal transduction pathway, was tested by pharmacological studies *in vitro* and *in vivo* by systemic administration in respective mouse models. mRNA-76 was found to prevent lung vascular leakage/lung edema as well as neutrophil infiltration in an LPS-challenging model.

Introduction

Acute respiratory distress syndrome (ARDS) is a life-threatening medical condition of respiratory failure characterized by rapid onset of widespread inflammation in the lungs. ARDS affects approximately 200 000 patients each year in the United States, and mortality and morbidity continues to be significant, remaining between 34.9 % and 40 %, depending on severity (Meyer et al. 2021; Matthay et al. 2019), resulting in nearly 75 000 deaths annually. Despite great improvements in management and heightened research efforts, ARDS still accounts for 10 % of intensive care unit (ICU) admissions globally, corresponding to more than 3 million patients with ARDS annually. ARDS can be caused by a variety of pulmonary (e.g., pneumonia, aspiration) or non-pulmonary (e.g., sepsis, pancreatitis, trauma) insults, leading to the development of nonhydrostatic pulmonary edema (Fan et al. 2018). Clinically, the syndrome is characterized by an acute developing, diffuse inflammatory lung injury initiated by increased alveolar capillary permeability, eventually resulting in increased lung weight, hypoxia (Fan et al. 2018) and fluid and neutrophil accumulation in the alveoli, which cannot be explained by hydrostatic edema. Primary treatment involves mechanical ventilation with low tidal volume together with treatments directed at the underlying cause, such as administering of antibiotics and fluid conservative strategies (Keddissi et al. 2019). However, to date there is no medication available for treatment and to further reduce ARDS mortality in patients. Hence there is a substantial medical need for novel and effective treatment approaches for ARDS, particularly in view of the significantly increased patient numbers affected by this life-threatening medical condition since onset of the worldwide “Covid-19” pandemic.

In ARDS, an initial vascular endothelial and alveolar epithelial cell activation or insult triggers massive liberation of inflammatory mediators, including complement activation products, cytokines, chemokines, proteases, and oxidants (Dolinay et al. 2012; Aranda-Valderrama and Kaynar 2018) which subsequently cause lung edema, a flooding of the lungs, thus impairing oxygen and carbon dioxide gas exchange of the lung capillaries. Albeit the inflammatory mediators recruiting immune cells, it is exactly their overabundance which eventually leads to a disruption of the endothelial barrier (vascular leakage) and to damage within the epithelial barriers in the alveolus. The endothelial angiopoietin (Ang)-Tie2 growth factor receptor pathway regulates vascular permeability and pathological vascular remodeling

(Saharinen et al. 2017b). Ang1 and Ang2 are both multimeric ligands for the receptor tyrosine kinase Tie2. In particular, the inactivation of Tie2 signaling due to an inflammatory increase in Ang2 secretion is regarded to be one of the major molecular mechanisms for the impairment of barrier function in the lung vasculature. Conversely, activation by Ang1 of Tie2 signaling restores endothelial barrier function and prevents further vascular leakage. This unique function of the Ang-Tie2 pathway in vascular stabilization renders this pathway an attractive and validated target in conditions such as ARDS, sepsis, macular edema, and cancer (Saharinen et al. 2017a).

Antibodies specific for Ang2 have been employed to prevent microvascular endothelial barrier dysfunction and to attenuate vascular remodeling and inflammation in a chronic lung infection model (Tabruyn et al. 2010). However, an Ang2 neutralization dependent restoration of basal Tie2 phosphorylation has not been shown so far. The second promising therapeutic approach to overcome Ang2 repression of the normal Tie2 signaling pathway has been to drive Tie2 activation to supra-physiological levels using recombinant Ang1 protein itself as well as derivatives thereof, such as COMP-Ang1 (Cho et al. 2004a) or CMP-Ang1 (Khan et al. 2021; Cho et al. 2004b). Additionally, either an unrelated agonist such as *Vasculotide* (Wu et al. 2015; Gutbier et al. 2017) or administration of cells expressing Ang1 (McCarter et al. 2007) were shown to be applicable and effective to that purpose. The approach to prevent and restore vascular barrier function by directly utilizing Ang1 proteins or derivatives has been hindered so far by the inherent predisposition of Ang1 to form higher order complexes for it to be catalytically active, since the Tie2 receptor only interact with highly oligomeric Ang1. Also, multimerization of Ang1 displays unfavorable pharmacokinetics. Highly oligomeric native Ang1 variants are, however, difficult to produce, purify and store in a stable and active form, and hence production in their multimeric form under GMP conditions has not been possible for clinical use so far. Recombinant COMP-Ang1 is a fusion protein comprised of the multimerization domain of the rat cartilage oligomeric matrix protein (COMP) combined with the fibrinogen-related domain of human Ang1 and has been described previously as a hyperactive Tie2 agonist.

Here, we describe the mRNA-based approach of directed expression and secretion of a hyperactive Ang1 derivative, hCOMP-hAng1 fusion protein, to transiently activate the Tie2 pathway *in vitro* and *in vivo*.

104 ## Materials & Methods

105 **mRNA synthesis**

106 Codon-optimized mRNAs encoding human Ang1, COMP-Ang1, CMP-Ang1, Tie2 and NanoLuc
107 proteins were synthesized and purified by BioSpring (Germany). Each mRNA was initiated
108 with a cap, followed by a 5′ untranslated region (UTR), a signal peptide sequence, an open-
109 reading frame (ORF) encoding Ang1, COMP-Ang1, CMP-Ang1 and Tie2, a 3′ UTR and a
110 polyadenylated tail. Uridine was globally replaced with 1-methylpseudouridine.

111

112 **Cell transfection *in vitro***

113 Hela cells were transfected with mRNAs using Lipofectamine MessengerMax (Invitrogen, cat.
114 #LMRNA001) according to manufacturer's protocol. Briefly, cells were seeded in 150 cm^2
115 culture flasks (TPP, cat. #90151) at 50 % confluency in serum-free DMEM (Gibco, cat.
116 #61965-026). 15 h later, cells were transfected for 2 h with indicated amounts of
117 MessengerMax-formulated mRNAs according to manufacturer's protocol. Transfection
118 media was removed and replaced with fresh serum-free DMEM for indicated time points.
119 After 24 h, the supernatant was removed (around 25 ml) and either concentrated 10-fold
120 with Amicon 3 kDa spin columns (Merck, cat. #UFC900308) and brought to a final volume of
121 2 ml for subsequent Western blot analysis (Fig.1B, C) or directly used for Tie2 activation
122 studies (Fig. 2A, B, Fig. 3B). Human pulmonary microvascular endothelial cells (HPMEC)
123 (Promocell, cat. #C-12281) were seeded onto 6-well plates (Thermo Scientific, cat. #140675)
124 and left for 3 days until 100 % confluency in full supplemented ECM MV2 cell media
125 (Promocell, cat. #C-22022). 15 h before transfection was placed in serum-reduced ECM MV2
126 media (containing 10 % of originally cell growth supplement MV2). Cells were transfected
127 with preformulated mRNA-LNP at indicated concentrations in serum-free ECM media for 2 h.
128 After transfection, media was replaced with serum-reduced ECM MV2 and left for indicated
129 time points.

130

131 **Western Blot analysis**

132 Cells were washed with ice-cold phosphate buffered saline (PBS) twice and lysed with ice-
133 cold RIPA buffer (Thermo Scientific, cat. #89901) supplemented with Halt™ Protease and
134 Phosphatase Inhibitor Cocktail (Thermo Scientific, cat. #78441). Tissue samples were

135 solubilized in T-PER™ Tissue Protein Extraction Reagent (Thermo Scientific, cat. #78510)
136 supplemented with Pierce Protease and Phosphatase Inhibitor tablets (Thermo Scientific,
137 cat. #A32958) using Qiagen TissueLyser LT (Qiagen, cat. #69980). A mixture of cell or tissue
138 lysate, 50 mM dithiothreitol NuPAGE reducing agent (Invitrogen, cat. #NP0009) and NuPAGE
139 sample buffer (Invitrogen, cat. #NP0007) were heated at 70 °C for 10 min, electrophoresed
140 in NuPAGE 4–12 % Novex Bis-Tris Gels and MOPS buffer (all from Invitrogen, cat.
141 #NP0335BOX, NP0001) and transferred to nitrocellulose membrane (Cytiva, cat. #10600003;
142 NuPAGE™ Transfer Buffer (Invitrogen, cat. #NP00061). After a 60 min blocking step
143 (Intercept® Blocking Buffer; LiCor, cat. #927-60001) membranes were washed with Tris
144 Buffered Saline with Tween® 20 (CST, cat. #9997S) probed at 4 °C overnight with specific
145 primary antibodies diluted in Intercept Antibody Diluent (LiCor, cat. #927-65001). Binding of
146 primary antibodies was detected by near infrared IRDye secondary antibodies (LiCor, cat.
147 #926-32213, 926-32214, 926-68072) and near infrared signals were analyzed using LiCor
148 Odysee CLx. Band intensities were analyzed using Empiria Studio Software 2.1.0134 (LiCor).
149 Primary antibodies used: Angiopoeitin 1 (abcam, cat. #ab183701), human Tie2 (CST, cat.
150 #7403), mouse Tie2 (Merck, cat. #05-584), pY992 Tie2 (R&D Systems, cat. #AF2720), Akt
151 (CST, cat. #9272 and #2920S), pS473 Akt (CST, cat. #4060), S6K (CST, cat. #9202), pT389 S6K
152 (CST, cat. #9234), FoxO1 (CST, cat. #2880), pT389 FoxO1 (CST, cat. #9461).
153
154 **Immunoprecipitation**
155 Anti-Tie2 antibody ab33 (R&D Systems, Merck, cat. #05-584) for Tie2 IP or Tie2-Fc fusion
156 protein (R&D Systems, cat. #313-TI) for COMP-Ang1 IP were covalently coupled to M-270
157 Epoxy Dynabeads™ (Thermo Scientific), cat. #14311D) at a ratio of 15 µg protein per mg
158 Dynabeads according to manufacturer's protocol. Briefly, 1.5 mg of antibody-coupled beads
159 were incubated with tissue lysates overnight at 4 °C. Beads were washed 5 times with 1 ml
160 with ice-cold RIPA buffer and finally denaturated using 1x NUPAGE loading dye containing 1x
161 NUPAGE reducing agent (all Thermo Scientific). Beads were removed and lysates were
162 analyzed by Western blotting analysis.
163
164 **Fluorescent microscopy**
165 HPMEC were seeded in Chamber Slides (NUNCTM Lab-TekTM, cat. #154534PK) at
166 $1x10^5$ cells/ml in endothelial MV2 growth medium. Cells were incubated for 3-5 days at 37°C

167 in 5 % CO_2. Cells were washed 2 times with pre-warmed PBS (Thermo Scientific, cat.
168 #14190), final PBS wash was replaced with endothelial MV2 basal medium devoid of serum
169 and supplements. Formulations containing mRNA were diluted in basal medium and added
170 to each well for a final concentration of 0,38 ng/well. Cells were returned to the incubator
171 for a further 2 hours. Media containing formulations was removed and replaced with 10 %
172 MV2 growth medium for 16 h. For TNFα treatment, 10 % MV2 growth medium with TNFα
173 (R&D Systems, cat. #210-TA) or vehicle was spiked into each well for a final concentration of
174 10 ng/ml for a further 6 h. Cells were fixed in 4 % PFA (Thermo Scientific, cat. #15670799) for
175 10 min at room temperature (RT). Cells were permeabilized in PBS containing 0.02 % Triton-
176 X (PBS-T) for 2x 10 min washes on a rocker at RT. Primary antibody mix was made up with
177 rabbit anti-VE-Cadherin (CST, cat. #2500) diluted at 1:400 in 2 % donkey immunobuffer
178 containing 0.02 % Triton-X, rocking at 4 °C overnight. Primary antibodies were removed and
179 washed in PBS-T 2x 10 min on a rocker at RT. Secondary antibody mix was made up with
180 donkey anti-rabbit (H+L) highly cross-adsorbed Alexa FluorTM 647 (Thermo Scientific, cat.
181 #A-31573) diluted at 1:400 and Alexa FluorTM 594 Phalloidin (Thermo Scientific, cat.
182 #A12381) at 1:2000 in 2 % donkey immunobuffer containing 0.02 % Triton-X rocking at RT
183 for 5 h. Cells were washed in PBS-T for a further 2x 10 min at RT. Nuclear staining was
184 carried out with Hoechst (Tocris, cat. #5117) diluted at 1:500 in PBS for 15 min, followed by a
185 final PBS-T wash. Fluorescent images were acquired with a Nikon Eclipse Ti-U with an ELWD
186 S Pan Fluor 40X/0.6 objective lens. Images were processed using ImageJ (Schneider et al.,
187 2012).
188
189 **Transcellular electrical resistance of human pulmonary microvascular endothelial cells**
190 HeLa cells were first treated for 24 h with LNP-formulated mRNA-76 or with a Luciferase
191 mRNA (see above) in order to generate conditional serum-free DMEM medium containing
192 secreted COMP-Ang1 or secreted luciferase. Moreover, HPMEC were grown to confluency
193 on evaporated gold microelectrodes (8-well array with ten electrodes per well, (ibidi GmbH,
194 cat. #72010) and connected to an Electrical cell-substrate impedance sensing system (ECIS;
195 Applied Biophysics, Troy, NY) (Tiruppathi et al. 1992; Giaever and Keese 1993) to enable
196 continuous monitoring of transcellular electrical resistance (TER) (Mitchell et al. 1989). After
197 monitoring baseline readings for 60-90 min, HPMEC medium was mixed 1:10 with the
198 conditional HeLa media (COMP-Ang1 supernatant or Luc supernatant) for 30 min or for

199 60 min before treatment with three different concentrations of pneumolysin (PLY; 0.25, 0.5
200 and 1.0 µg/ml) (Mitchell et al. 1989) to evoke a barrier failure in HPMEC. TER values from
201 each microelectrode were continuously monitored for 5 hours after PLY stimulation and
202 normalized as the ratio of measured resistance to baseline resistance. The area under the
203 curve (AUC) was calculated from start of PLY stimulation on.
204
205 **Animals**
206 Female C57BL/6N mice (8 to 10 weeks, 18 to 20 g; Charles River, Sulzfeld, Germany) were
207 used for all experiments. All animal experiments were approved by institutional and
208 governmental German authorities ("Tierschutzbeauftragte" (animal welfare officer) and
209 "Tierschutzausschuss" of Charité–Universitätsmedizin Berlin; and by the Landesamt für
210 Gesundheit und Soziales Berlin; approval ID A0179/20), and were in accordance with the
211 Federation of European Laboratory Animal Science Associations (FELASA) guidelines and
212 recommendations for the care and use of laboratory animals (equivalent to American
213 ARRIVE). Mice were randomly assigned to the appropriate experimental groups and were
214 kept in closed, individually ventilated cages with filter hoods (type II-L, ZOONLAB), under
215 specific pathogen-free conditions, with free access to food and water, room temperature
216 between 20 and 22 °C, air humidity between 50 and 65 % and 12 h light/dark cycle.
217
218 **Transfection in vivo and isolated perfused and ventilated mouse lung (IPML) experiments**
219 Intravenous tail vein administration (slow 100 µl bolus tail vein injection) with either
220 Luciferase-mRNA (2 mg/kg) or mRNA-76 (2 mg/kg, 1.5 mg/kg or 1 mg/kg) was performed 6 h
221 or 15 h before the experiment in the isolated mouse lung model was started. Subsequently,
222 mice were anesthetized, placed in a 37 °C heated chamber ("artificial thorax"),
223 tracheotomized and ventilated as described (Von Bethmann et al. 1998). After laparotomy,
224 final blood collection via the vena cava, sternotomy, and cannulation (pulmonary artery, left
225 atrium), lungs were perfused with Krebs-Henseleit-hydroxyethylamylopectine buffer (Serag-
226 Wiessner) supplemented with sodium bicarbonate (1:50). The chamber was closed, and
227 lungs were ventilated by negative pressure (Pexp -4.5, Pins -9.0 cm H_2O) and perfused
228 (1 ml/min) for 20 min to establish baseline conditions. Then 0.04 % human serum albumin
229 (HSA; 20 % solution; CSL Behring, cat. #Human-Albumin 20 % Behring) was admixed
230 continuously to the perfusate 10 min prior to intravenous bolus application of recombinant

231 pneumolysin (PLY; 1.4 µg/ml) (Mitchell et al. 1989). Thirty minutes after PLY challenge,
232 bronchoalveolar lavage (BAL) was performed (2 x 650 µl, 0.9 % saline buffer), and HSA
233 concentration was measured in BAL fluid (BALF) via ELISA (Bethyl Laboratories, cat. #E88-
234 129) in order to quantify the lung barrier failure (Seybold et al. 2005; Witzenrath et al. 2006).
235

236 **Neutrophilia transmigration experiment**

237 Animals (n=10) were challenged intratracheally with 0.9 % w/v saline or with LPS (3 mg/kg).
238 Two hours later animals were treated with mRNA-76-cLNP or with control $mRNA^{LUC}$-cLNP
239 employing a dosage of 1.5 mg/kg via intravenous tail vein injection. Control group animals
240 received intraperitoneal injections of Dexamethasone (3 mg/kg) one hour prior to, and 8
241 hours after LPS administration. Animals were sacrified after 24 hours and the airway lavaged
242 with 0.3 ml of PBS using an inserted cannula. The bronchoalveolar lavage from each mouse
243 was centrifuged at 1000 g for 10 min at ca 4 °C. The cell pellet was re-suspended in 0.5 ml
244 PBS and retained on wet ice until analysis. A total and differential cell count of the BALF
245 supernatant was performed using the XT-2000iV (Sysmex UK Ltd). The samples were
246 vortexed for approximately 5 seconds and analyzed. Total and differential cell counts
247 (including neutrophils, lymphocytes and mononuclear cells (includes monocytes and
248 macrophages)) were measured as number of cells per animal.
249

250 ## Results

251 Expression of coding sequences of the wild-type human Ang1 and of engineered fusion
252 proteins COMP-Ang1 and CMP-Ang1 flanked by heterologous untranslated regulatory
253 sequences was tested in cell culture systems in order to identify a potent mRNA construct
254 for Tie2 activation. Wildtype human Ang1 mRNA with heterologous UTRs served as a control
255 next to either a construct with an ORF for a COMP-Ang1 fusion protein or a construct
256 containing an ORF with a CMP-Ang1 fusion protein (**Fig. 1A**). Similar COMP-Ang1 and CMP-
257 Ang1 recombinant fusion proteins have been previously described which contain the rat
258 homologue of COMP or human CMP as potent Tie2 agonist in *in vitro* assays and in mouse
259 models (Cho et al. 2004b; Oh et al. 2015; Wallace et al. 2021).
260

261 **mRNA directs transient expression of human Ang-1 and COMP-Ang1 and CMP- fusion**
262 **proteins *in vitro***

263 *mRNAs* encoding wildtype human Ang1, fusion proteins COMP-Ang1 and CMP-Ang1 were
264 transfected into HeLa cells using Lipofectamine MessengerMax. Cell culture supernatants
265 were collected 3 h, 6 h and 24 h after the transfection, and corresponding whole cell lysates
266 were prepared. The supernatants and cell lysates were subsequently analyzed by
267 immunoblotting employing an Ang-1 specific antibody. A strong protein expression signal
268 was detected for all three constructs, and protein levels post-transfection of the mRNA
269 construct were found to be higher than those of endogenous Ang-1 protein (**Fig. 1B**).
270 Equivalent protein levels were detected in the supernatant of the cell culture, indicating
271 secretion of the expressed proteins (**Fig. 1C**). Multimerization potential of the expressed
272 Ang1 derivates was analyzed by employing non-reducing PAGE on the supernatant. Contrary
273 to CMP-Ang1, the COMP-Ang1 fusion protein was found to be capable of forming higher-
274 order (pentameric) homopolymers (**Fig. 1D**).
275

276 **Activation of Tie2 by COMP-Ang1 and CMP-Ang1**

277 The chimeric COMP-Ang1 derivative encoded by mRNA-76 was found to *in vitro* activate Tie2
278 in a paracrine manner. Tie2-negative HeLa cells were first transfected for 24 h with *mRNA*
279 encoding for Tie2 receptor using Lipofectamine MessengerMax. Subsequently, cells were
280 incubated for 15 min or 30 min with supernatants from HeLa cells previously transfected for
281 24 h with mRNA encoding the different Ang1 derivatives, or with NanoLuc-encoding control
282 mRNA using Lipofectamine MessengerMax. Ensuing, Tie2-transfected HeLa cells were lysed
283 and protein levels analyzed by Western blotting. Both supernatants with Ang1 derivatives
284 displayed a significantly stronger activation of the Tie2 receptor as assessed by phospho-
285 Y992 Tie2 antibody (**Fig. 2A**) than when activated by the Luc-control and wildtype Ang1
286 proteins. Ability of different Ang1-derivatives to induce paracrine activation of the Tie2
287 pathway in human primary endothelial cells was then investigated in a second set of
288 experiments. For this, starved primary HPMECs (human primary microvascular endothelial
289 cells) were incubated for 10 and for 30 min with supernatants from HeLa cells previously
290 transfected in serum-free medium for 24 h with mRNAs encoding the different Ang1
291 derivatives using Lipofectamine MessengerMax, or with NanoLuc as a control. HPMEC cells
292 were lysed after 10 and 30 min, and phosphorylation status of Tie2, Akt and S6K analyzed by

293 Western blotting and compared to lysates from starved cells or from cells stimulated for 10
294 and 30 min with FCS (**Fig. 2B**). Strongest downstream activation of Akt and S6K was seen
295 with FCS treatment on starved cells, thus corroborating the expected broad growth factor
296 response. Cells treated with supernatant from HeLa cells transfected with mRNA-76
297 encoding COMP-Ang1 also showed robust phosphorylation of Akt and of S6K, but
298 additionally exhibited autophosphorylation of Tie2, indicative for a more specific pathway
299 activation. The paracrine effect of HeLa conditional medium-derived COMP-Ang1 resulted in
300 a better Tie2 pathway activation as compared to CMP-Ang1, leading to selection of mRNA-
301 76 /COMP-Ang1 for the following experiments. mRNA-76 encoding COMP-Ang1 was directly
302 transfected into HPMEC and secretion and Tie2 signaling was analyzed in order to
303 demonstrate increased autocrine Tie2 activation. Strong COMP-Ang1 expression was
304 observed in cell lysates and in the supernatant of the respective culture, indicating efficient
305 secretion (**Fig. 2C**). Lysate analysis of serum-starved HPMEC transfected with mRNA-76
306 revealed phosphorylation of Tie2, Akt and FOXO1, thereby indicating functional Tie2
307 pathway activation at 4 h and 8 h post-transfection, as well as fast onset of activation.
308 Waning of Tie2 receptor activation and a reduction of Tie2 receptor protein was observed at
309 24 h and 48 h post transfection, consistent with previous reports describing a ligand
310 dependent Tie2 internalization and degradation (Bogdanovic et al. 2006; Ghosh et al. 2016;
311 Wehrle et al. 2009) as well as reduced expression of Tie2 mRNA upon Ang1 treatment
312 (Hashimoto et al. 2004).
313
314 **COMP-Ang1 expression stabilizes endothelial barrier function *in vitro***
315 Regulation of endothelial barrier stabilization by Ang1/Tie2 signaling has been shown to be
316 mediated by VE-Cadherin-dependent cell-cell adhesion and cortical actin formation, since
317 the cytoplasmatic tail of VE-cadherin is known to contain several phosphorylation sites with
318 different distinctive and selective effects on endothelial cell function (Hellenthal et al. 2022).
319 However, inflammatory conditions lead to disruption of VE-Cadherin complexes by
320 phosphorylation-dependent internalization and by degradation, as well as to formation of
321 actin stress fibers. We analyzed VE-Cadherin distribution in HPMEC cells upon TNFα
322 challenge by immunofluorescence staining and by microscopy analysis.
323 As reported previously (Xia et al. 1998), TNFα was shown to induce disruption of cell-cell
324 adhesion as verified by disruption intercellular VE-Cadherin staining (**Fig. 3A**, arrows) and by

325 formation of actin stress fibers in non-transfected cells (UT) as well as in cells transfected
326 with control mRNA^{LUC}-cLNP. However, cells transfected with mRNA-76-cLNP displayed more
327 VE-Cadherin staining even if unstimulated but in the presence of TNFα. This observation
328 argues for the existence of increased VE-Cadherin trans-interaction area at overlapping cell
329 edges, as previously also described by Birkuva *et al.* (Birukova et al. 2012).
330 Following demonstration of functional Tie2 activation on VE-Cadherin complex stabilization,
331 we investigated the potential effect of mRNA-76 directed expression of COMP-Ang1 on
332 pneumolysin-evoked barrier failure in cell culture. Recovery of the pneumolysin-evoked
333 barrier failure was measured by monitoring transcellular electrical resistance (TER)
334 (Srinivasan et al. 2015). TER measurements are performed by applying an AC electrical signal
335 across electrodes placed on both sides of a cellular monolayer and subsequently measuring
336 voltage and current to calculate the electrical resistance of the barrier (Elbrecht et al. 2016).
337 A significantly improved transcellular electrical resistance was observed with the mRNA-76
338 conditional medium at lowest pneumolysin concentration of 0.25 µg/ml, but not with the
339 supernatant form HeLa cells transfected with Luciferase mRNA (**Fig. 3B,** purple lines: COMP-
340 Ang1 dotted line, Luciferase supernatant solid line). This effect was observed in
341 pneumolysin-induced barrier failure experiments after pretreatment with conditional
342 supernatant for 30 min or 60 min. These data indicate that mRNA-76 treatment leads to
343 expression and secretion of COMP-Ang1 and the so expressed COMP-Ang1 is functional in a
344 paracrine manner on microvascular endothelial cell (HPMEC) monolayers as demonstrated
345 by its ability to attenuate the PLY-induced TER decrease. These findings confirm the
346 proposed mode of action of our COMP-Ang1 molecule in diminishing inflammation induced
347 hyperpermeability via its respective activation of the Tie2 signaling pathway.
348
349 **mRNA-76 enables COMP-Ang1 expression and Tie2 pathway activation in mice**
350 Various physical characteristics of LNPs affect organ biodistribution and cell specificity of the
351 mRNA delivery, namely size, surface charge, pKa of the lipids, lipid composition and
352 mRNA/lipid ratio, PEGylation (Eygeris et al. 2022; Hou et al. 2021; Kauffman et al. 2016;
353 Kowalski et al. 2019). We show that our mRNA-76 formulated in cationic lipid-nanoparticles
354 (cLNPs) enable Tie2 activation by paracrine and autocrine COMP-Ang1 expression *in vivo.*
355 Our cationic LNP formulations are based on lipoplex formulations previously described, for
356 siRNA *in vivo* delivery to the pulmonary endothelium (Fehring et al. 2014; Gutbier et al.

357 2018; Santel et al. 2006b, 2006a). Expression of mRNA-76 directed COMP-Ang1 was analyzed
358 by Western Blot of protein from lung tissue from mice (n=4) treated by intravenous tail vein
359 administration with 2 mg/kg mRNA-76-cLNP. Robust COMP-Ang1 expression was detected in
360 lung lysates from mice 6 h after treatment, and declining expression levels were observed in
361 mice 24 h post treatment due to the transient nature of mRNA (**Fig. 4A**). As expected from
362 previous studies with cationic LNPs, mRNA-76-cLNP mediated robust lung tissue-selective
363 COMP-Ang1 expression, while inducing no significant COMP-Ang1 expression in tissue
364 lysates from heart, liver, spleen, and kidney (**Fig. 4B**). Immune-precipitation was performed
365 on different organ lysates using Tie2-Fc fusion protein for capturing of COMP-Ang1 to
366 confirm lung selective COMP-Ang1 expression. Even with this more sensitive detection
367 method the predominant COMP-Ang1 expression was observed in lung lysates, with some
368 minor expression also seen in the spleen (**Fig. 4C**). No significant expression of COMP-Ang1
369 was detected in liver, heart and kidney thus confirming the selective pulmonary delivery of
370 mRNA-76-cLNP.
371
372 **Single-cell transcriptomics of murine lungs after mRNA-76-cLNP treatment**
373 We performed single-cell RNA-sequencing on cells derived from murine lungs in order to
374 characterize the specific cell types with mRNA-76 uptake. Lungs from two mice treated with
375 1.5 mg/kg mRNA-76-cLNP (2 h post administration) were obtained, and lung cell suspension
376 was subjected to droplet-based single-cell gene expression profiling (**Fig. 5A**). We obtained
377 5,100 high-quality transcriptome readings and were able to identify 13 cell clusters with
378 main cell types of the respective lung samples by employing dimensionality reduction via t-
379 distributed stochastic neighbor embedding (t-SNE) and graph-based clustering (**Fig. 5B**).
380 We observed mRNA-76 reads to be largely restricted to cluster 8 and cluster 10,
381 representing cells of the alveolar capillary endothelium (gCap, general capillary cells) and
382 aCap (alveolar capillary cells) recently termed aerocytes (Gillich et al. 2020), as well as
383 monocytes, respectively. Minor amounts of mRNA-76 appeared to also be present in a sub-
384 cluster of the pulmonary neutrophils (cluster 11). We analyzed the mRNA reads of Tie2 and
385 VE-cadherin, both being endothelial cell specific expressed genes, in order to confirm the
386 endothelial specific clustering for mRNA-76 into cluster 8. The overlap with the reads for
387 both markers confirmed cell type specificity of mRNA-76 delivery (**Fig. 5D**). In contrast to
388 mRNA-76, endogenous Ang1 mRNA is mainly detected in cluster 6, which does not overlap

389 with reads for the Tie2 receptor mRNA (**Fig. 5E**). The observed cell type-specific expression
390 profiles suggest a paracrine Tie2 activation for the endogenous Ang1, as well as a potential
391 autocrine Tie2 activation by ectopically expressed, mRNA-76-encoded COMP-Ang1.
392
393 **mRNA-76 mediated Tie2 pathway activation in murine lungs**
394 We then demonstrated Tie2 pathway activation in lung tissue to be induced by mRNA-76
395 COMP-Ang1 expression in murine lung tissue. Activation of PI3 kinase signaling including Akt
396 phosphorylation is known to be a downstream effect of Tie2 receptor activation. Of note,
397 demonstrating COMP-Ang1 mediated activation of Tie2 signaling is difficult due to the low
398 proportion of Tie2-expressing endothelial cells within total lung lysates in healthy, non-
399 inflamed lungs. Therefore, Tie2 was immuno-precipitated from lung tissue lysates of mice
400 previously treated with mRNA-76 using Tie2-specific antibodies. Tie2 phosphorylation of the
401 lung was subsequently shown by Western blot analysis of immuno-precipitated samples
402 using anti-phospho-Tie2 antibody (p*Y992) (**Fig. 6A**). Signal quantification of phosphorylated
403 Tie2 was performed using LiCor Odyssee CLx and measured relative to corresponding total
404 Tie2 levels. In addition, immunoblot analysis using Ang1-specific antibodies showed co-
405 immunoprecipitation of COMP-Ang1 thus demonstrating efficient binding of human COMP-
406 Ang1 to murine Tie2. Since Akt phosphorylation upon COMP-Ang1 stimulation is mediated
407 by Tie2 activation, whole lung tissue lysates from mice treated with 1.5 mg/kg mRNA-76-
408 cLNP were analyzed for COMP-Ang-1 expression, Akt expression and Akt-phosphorylation by
409 immunoblot (**Fig. 6B**) in comparison to control lysates (Saline treated). Akt phosphorylation
410 levels were shown to be highest 6 h post mRNA-76-cLNP treatment.
411
412 **mRNA-76 treatment reduces pneumolysin-evoked vascular permeability in an isolated**
413 **perfused and ventilated mouse lung (IPML) model for vascular leakage**
414 A pneumolysin (PLY) stimulation experiment was performed on isolated and ventilated
415 mouse lungs (IPML model) to demonstrate mRNA-76 efficacy in preventing and/or
416 decreasing lung hyperpermeability by inflammation (**Fig. 7A**). In the employed IPML model,
417 PLY stimulation increases lung permeability 30 min after application, as described previously
418 (Gutbier et al. 2017; Witzenrath et al. 2006). Here, treatment with mRNA-76 significantly
419 decreased pneumolysin-induced hyperpermeability of mouse lungs as compared to
420 treatment with Luciferase (**Fig. 7B**). Dose dependent reduction of HSA levels in the BALF was

observed at 6 h and 15 h post mRNA-76 treatment as compared to that derived from control mice, indicating reduced vascular leakage. These results suggest that mRNA-76 pretreatment is effective in preventing pneumolysin-induced vascular leakage in the IPML model, and respective observations are consistent with the previously established mode of action of Tie2 activation by mRNA-76 directed expression of COMP-Ang1 in lung tissues. The effective dose in this mouse efficacy model is approx. 1 mg/kg for the 6 h time point and marginally higher at later time points (15 h). This decreasing effect on vascular leakage at later time points with lower doses suggests a more sustained expression with higher mRNA-76 dosing.

mRNA-76 directed COMP-Ang1 expression reduces neutrophil influx after LPS challenge in murine lungs

We observed a significant therapeutic effect on endotoxin/LPS induced neutrophilia after temporal and spatial expression of COMP-Ang1 in a murine model of endotoxin (*E. coli* lipopolysaccharide, LPS)-induced pulmonary inflammation (**Fig. 8A**). Hence, we detected a significant decrease in LPS induced neutrophil influx into the alveoli after single mRNA-76-cLNP treatment in our experimental model (**Fig. 8B**). The level of the decreased neutrophil influx effect is in the same range as that of prophylactic and therapeutic dexamethasone treatment used as positive control for this assay. No significant reduction regarding cell influx was observed with $mRNA^{Luc}$-cLNP as compared to vehicle control mice. Also, no changes in LPS induced vascular leakage (e.g., changes in wet lung weights) were observed with mRNA-76-cLNP treatment as compared to control mRNA formulation, indicating that vascular leakage and leucocyte emigration do not necessarily occur together in the blood vessels of the lung. The fact that elevated levels of circulating cytokines are not perturbed by enhancement of vascular integrity and hence the notion that leakage can be regulated distinctly from the inflammatory response has been discussed previously by others (Filewod and Lee 2019). Generally, the effect of mRNA-76-cLNP treatment in rodent models for LPS-induced lung injury could also be dependent on the time point at which samples are obtained, and at which respective physiological measurements are taken. The LPS model might therefore be not adequate to simultaneously address the question of both neutrophil efflux as well as lung edema at similar timepoints 24 h post endotoxin challenge, as opposed to the IPML model which was used primarily for experimentally reducing vascular leakage. In our in a murine model of LPS-induced pulmonary inflammation, intravenous mRNA-76-cLNP

453 treatment showed a strong therapeutic effect in reducing leukocyte extravasation and/or
454 transmigration of neutrophils for the timepoint(s) analysed. Notably, leukocyte influx
455 reduction and reduction in edema formation might be clinically highly desirable to
456 counteract delayed apoptosis of parenchymal neutrophils, believed to contribute to tissue
457 injury (Teder et al. 2002). Taken together, our experiments in the IPML mouse model
458 confirm a dose dependent therapeutic effect of COMP-Ang1 on endothelial permeability, as
459 well as a therapeutic efficacy on dysregulated lung inflammation in the LPS-induced
460 pulmonary neutrophilia mouse model. Both underlying pathophysiological mechanism, loss
461 of endothelial permeability and dysregulated lung inflammation, are hallmark events of early
462 ARDS syndrome.

463

464 **Discussion**

465 In our work presented here we introduce mRNA-76-LNP, a novel drug modality utilizing
466 mRNA-based expression technology, in combination with a lipid nanoparticle-based delivery
467 technology, to achieve transient and localized expression of functional Ang1 protein
468 derivatives in the lung vasculature. Our new approach and technology thus overcome the
469 limitations of efficaciously administering recombinant multimeric proteins for activating Tie2
470 signaling. For example, full-length Ang1 unlike Ang2, has been shown previously by Xu et al.
471 to be incorporated efficiently into the extracellular matrix (ECM) via its linker peptide region,
472 thereby explaining its rapid serum clearance. Interestingly, in our experiments, only COMP-
473 Ang1 and CMP-Ang1 were detected in significant amounts in the cell supernatant, thus
474 indicating efficient secretion (**Fig. 1C**). This is in contrast to the comparably high intracellular
475 expression levels in lysates of HeLa cells transfected with the three Ang1 variants (**Fig. 1B**).
476 One possible explanation for this observed difference might be that albeit the Ang1 linker
477 domain being present in all three Ang1 variants, conceivably only wt-Ang1 interacts with
478 components of the ECM via its N-terminal multimerization domain. Moreover, COMP-Ang1
479 and CMP-Ang1 show a more robust Tie2 activation in Hela cells with high levels of
480 ectopically expressed Tie2, hence suggesting a superior paracrine activity of COMP-Ang1 and
481 CMP-Ang1 as compared to wt-Ang1. In fact, paracrine Tie2 activation was demonstrated
482 only with COMP-Ang1 in HPMEC. COMP-Ang1 was shown to form solely pentamers, this

483 being most likely due to the presence of the COMP multimerization domain. In contrast,
484 CMP-Ang1 was shown to preferentially form dimers owing to the presence of its CMP
485 dimerization domain (**Fig. 1D**). Tie2 activation has been previously reported to require a
486 specific distance of the Ang1 binding domains in relation to the two Tie2 monomers
487 (Leppänen et al. 2017). This very specific steric/spatial interaction is potentially facilitated by
488 the pentameric COMP-Ang1 as compared to the dimeric CMP-Ang1 in low Tie2 expressing
489 HPMEC cells. As a result ,the observed higher and robust COMP-Ang1 mediated Tie2
490 activation in our system is most likely caused by its higher solubility compared to wt-Ang1, as
491 well as by its more efficient multimerization into active pentamers as compared to that of
492 CMP-Ang1. The difference in Tie2 activation (**Fig. 2**) in our hands led us focus on mRNA-76
493 encoding COMP-Ang1 for our further experiments. We subsequently demonstrated that
494 mRNA-76 mediated COMP-Ang1 expression and Tie2 activation had phenotypic effects on
495 cell adhesion by way of monitoring transcellular electrical resistance in HPMEC monolayers
496 (**Fig. 3**). This observed stabilization of endothelial barrier function in *in vitro* cell culture is
497 consistent with our *in vivo* results demonstrating a reduction of pneumolysin-evoked
498 permeability in isolated perfused and ventilated mouse lungs after mRNA-76 treatment (**Fig.**
499 **6**). The underlying LNP formulation used in these experiments is based on our previous
500 experimental work with siRNA-lipoplex formulations (Fehring et al. 2014; Santel et al. 2006b,
501 2006a). Functional delivery of the mRNA-76 payload was shown to occur in the lung
502 vasculature, more specifically in pulmonary capillary endothelial cells (scRNA-Seq **Fig. 5**).
503 Hence, here the synthetic mRNA becomes translated and consequently respective COMP-
504 Ang1 is secreted as a multimer in order to bind and activate Tie2 receptors in a presumably
505 paracrine and autocrine rather than endocrine manner (**Fig. 4**). Our data demonstrating
506 COMP-Ang1 expression in mouse lung tissue together with *in vivo* mRNA-76 uptake by single
507 cell transcriptional analysis and its subsequent Tie2 pathway activation in moues lung tissue
508 therefore demonstrate the projected mode of action of our novel mRNA-76-cLNP
509 compound. Data in **Fig. 9 B** show a significant decrease in LPS induced neutrophil influx into
510 the alveoli after **s**ingle mRNA-76-cLNP treatment. We did not observe changes in LPS
511 induced vascular leakage (e.g., changes in wet lung weights) with mRNA-76-cLNP when
512 compared to control mRNA formulation in this model. These data may indicate that vascular
513 leakage and leucocyte extravasation do not necessarily occur together in blood vessel of the
514 lung, which has been discussed previously by others (Filewod and Lee 2019). Generally,

515 these findings in murine models for LPS-induced lung injury may also depend on the time
516 point at which samples are obtained and the corresponding physiological data are captured.
517 In contrast to the IPML model for primarily addressing vascular leakage, the LPS model might
518 be not adequate for simultaneously addressing both neutrophil efflux and lung edema at
519 24 h post endotoxin challenge. Intravenous mRNA-76-cLNP treatment was shown to
520 intervene with leukocyte and in particular neutrophil extravasation into the alveoli after LPS
521 challenge. It should be noted however, that the reduction of the influx of leukocytes in
522 addition to a reduction in edema formation might be clinically highly desirable to counteract
523 the delayed apoptosis of parenchymal neutrophils believed to contribute to tissue injury
524 (Teder et al. 2002).
525 Taken together the data in our IPML mouse model demonstrate a dose dependent
526 therapeutic effect of mRNA-76-cLNP regarding endothelial permeability, while the LPS-
527 induced pulmonary neutrophilia mouse model depicted in **Fig. 9**. shows therapeutic efficacy
528 on dysregulated lung inflammation. Both underlying pathophysiological mechanisms, namely
529 loss of endothelial permeability and dysregulated lung inflammation, are hallmark events at
530 the onset of early/ mild ARDS. Thus, the advantage of our novel mRNA-76-cLNP compound
531 as described above is its ability to act in a highly spatially restricted manner thereby enabling
532 the Tie2 agonist to rapidly and almost exclusively target specifically that site of the
533 endothelial capillary bed where the pathophysiological lung edema occurs. This particular
534 strong spatial restriction of action of our mRNA compound enables a more rapid onset of
535 Tie2 pathway activation, as well as improved pharmacodynamics, compared to those drug
536 modalities which require a more continuous treatment due to the rapid clearance of
537 recombinant proteins from the systemic circulation. Increased Ang2 levels were also found
538 more recently to be strongly associated with COVID-19 in-hospital mortality and with non-
539 resolving pulmonary condition (Villa et al. 2021a). Thus, Ang2 may be an early and useful
540 predictor and biomarker for patient stratification and of the clinical course of COVID-19, and
541 impending Ang2 binding a potential treatment option against COVID-19 (Villa et al. 2021b).
542 Moreover, inhibition of the antagonistic Ang2 or a transient and localized upregulation of
543 Ang1 -or a hyperactive derivative thereof- is a promising strategy to restore Tie2 signaling in
544 order to stabilize the barrier function and to prevent the inflammatory lung leakage in
545 ARDS/COVID-19 patients. With the understanding that the angiopoietin/Tie (Ang/Tie) family
546 has an established role in vascular physiology in regulating angiogenesis, vascular

permeability, and inflammatory responses, our data corroborate effectiveness and mode of action of the clinical approach of treating damage of the lung vascular epithelium with transient expression of an mRNA-LNP modality. The highly specific targeting of our respective COMP-Ang1 cationic LNP of the lung vasculature thus enables spatially highly restricted expression of COMP-Ang-1 for treating edema formation in ARDS patients as a new treatment modality for further development.

554 **References**

555 Aranda-Valderrama P, Kaynar AM. 2018. The Basic Science and Molecular Mechanisms of
556 Lung Injury and Acute Respiratory Distress Syndrome. *International anesthesiology*
557 *clinics* **56**: 1. /pmc/articles/PMC7680967/ (Accessed September 27, 2022).
558 Bogdanovic E, Nguyen VP, Dumont DJ. 2006. Activation of Tie2 by angiopoietin-1 and
559 angiopoietin-2 results in their release and receptor internalization. *J Cell Sci* **119**: 3551–
560 3560. https://www.ncbi.nlm.nih.gov/pubmed/16895971.
561 Calfee CS, Gallagher D, Abbott J, Thompson BT, Matthay MA. 2012. Plasma angiopoietin-2 in
562 clinical acute lung injury: prognostic and pathogenetic significance. *Critical care*
563 *medicine* **40**: 1731–1737. https://pubmed.ncbi.nlm.nih.gov/22610178/ (Accessed
564 September 27, 2022).
565 Cho CH, Kammerer RA, Lee HJ, Steinmetz MO, Ryu YS, Lee SH, Yasunaga K, Kim KT, Kim I,
566 Choi HH, et al. 2004a. COMP-Ang1: A designed angiopoietin-1 variant with nonleaky
567 angiogenic activity. *Proceedings of the National Academy of Sciences of the United*
568 *States of America* **101**: 5547–5552.
569 https://www.pnas.org/doi/abs/10.1073/pnas.0307574101 (Accessed September 26,
570 2022).
571 Cho CH, Kammerer RA, Lee HJ, Yasunaga K, Kim KT, Choi HH, Kim W, Kim SH, Park SK, Lee
572 GM, et al. 2004b. Designed angiopoietin-1 variant, COMP-Ang1, protects against
573 radiation-induced endothelial cell apoptosis. *Proceedings of the National Academy of*
574 *Sciences of the United States of America* **101**: 5553–5558.
575 https://www.pnas.org/doi/abs/10.1073/pnas.0307575101 (Accessed September 26,
576 2022).
577 Diamond JM, Porteous MK, Cantu E, Meyer NJ, Shah RJ, Lederer DJ, Kawut SM, Lee J,
578 Bellamy SL, Palmer SM, et al. 2012. Elevated plasma angiopoietin-2 levels and primary
579 graft dysfunction after lung transplantation. *PloS one* **7**.
580 https://pubmed.ncbi.nlm.nih.gov/23284823/ (Accessed September 27, 2022).
581 Dolinay T, Kim YS, Howrylak J, Hunninghake GM, An CH, Fredenburgh L, Massaro AF, Rogers
582 A, Gazourian L, Nakahira K, et al. 2012. Inflammasome-regulated cytokines are critical
583 mediators of acute lung injury. *American journal of respiratory and critical care*
584 *medicine* **185**: 1225–1234. https://pubmed.ncbi.nlm.nih.gov/22461369/ (Accessed
585 September 27, 2022).
586 Elbrecht DH, Long CJ, Hickman JJ. 2016. Transepithelial/endothelial Electrical Resistance
587 (TEER) theory and ap-plications for microfluidic body-on-a-chip devices Keywords TEER
588 Body-on-a-chip Barrier tissue Blood-brain barrier Organ Endothelial cells Epithelial cells
589 Human-on-a-chip. *J Rare Dis Res Treat* **1**: 46–52. www.rarediseasesjournal.com
590 (Accessed September 28, 2022).
591 Eygeris Y, Gupta M, Kim J, Sahay G. 2022. Chemistry of Lipid Nanoparticles for RNA Delivery.
592 *Acc Chem Res* **55**: 2–12. https://www.ncbi.nlm.nih.gov/pubmed/34850635.
593 Fan E, Brodie D, Slutsky AS. 2018. Acute Respiratory Distress Syndrome: Advances in
594 Diagnosis and Treatment. *JAMA* **319**: 698–710.
595 https://jamanetwork.com/journals/jama/fullarticle/2673154 (Accessed September 27,
596 2022).
597 Fehring V, Schaeper U, Ahrens K, Santel A, Keil O, Eisermann M, Giese K, Kaufmann J. 2014.
598 Delivery of therapeutic siRNA to the lung endothelium via novel Lipoplex formulation
599 DACC. *Molecular therapy: the journal of the American Society of Gene Therapy* **22**:

811–820. https://pubmed.ncbi.nlm.nih.gov/24390281/ (Accessed September 26, 2022).
Filewod NC, Lee WL. 2019. Inflammation without Vascular Leakage. Science Fiction No Longer? *Am J Respir Crit Care Med* **200**: 1472–1476. https://www.ncbi.nlm.nih.gov/pubmed/31381867.
Gallagher DC, Bhatt RS, Parikh SM, Patel P, Seery V, McDermott DF, Atkins MB, Sukhatme VP. 2007. Angiopoietin 2 is a potential mediator of high-dose interleukin 2-induced vascular leak. *Clinical cancer research: an official journal of the American Association for Cancer Research* **13**: 2115–2120. https://pubmed.ncbi.nlm.nih.gov/17404094/ (Accessed September 27, 2022).
Gallagher DC, Parikh SM, Balonov K, Miller A, Gautam S, Talmor D, Sukhatme VP. 2008. Circulating angiopoietin 2 correlates with mortality in a surgical population with acute lung injury/adult respiratory distress syndrome. *Shock (Augusta, Ga)* **29**: 656–661. https://pubmed.ncbi.nlm.nih.gov/18091573/ (Accessed September 27, 2022).
Ghosh CC, David S, Zhang R, Berghelli A, Milam K, Higgins SJ, Hunter J, Mukherjee A, Wei Y, Tran M, et al. 2016. Gene control of tyrosine kinase TIE2 and vascular manifestations of infections. *Proc Natl Acad Sci U S A* **113**: 2472–2477. https://www.ncbi.nlm.nih.gov/pubmed/26884170.
Giaever I, Keese CR. 1993. A morphological biosensor for mammalian cells. *Nature* **366**: 591–592. https://www.ncbi.nlm.nih.gov/pubmed/8255299 (Accessed September 29, 2022).
Gillich A, Zhang F, Farmer CG, Travaglini KJ, Tan SY, Gu M, Zhou B, Feinstein JA, Krasnow MA, Metzger RJ. 2020. Capillary cell-type specialization in the alveolus. *Nature* **586**: 785–789. https://www.ncbi.nlm.nih.gov/pubmed/33057196.
Gutbier B, Jiang X, Dietert K, Ehrler C, Lienau J, Van Slyke P, Kim H, Hoang VC, Maynes JT, Dumont DJ, et al. 2017. Vasculotide reduces pulmonary hyperpermeability in experimental pneumococcal pneumonia. *Critical Care* **21**.
Gutbier B, Neuhauß AK, Reppe K, Ehrler C, Santel A, Kaufmann J, Scholz M, Weissmann N, Morawietz L, Mitchell TJ, et al. 2018. Prognostic and pathogenic role of angiopoietin-1 and -2 in pneumonia. *American Journal of Respiratory and Critical Care Medicine* **198**: 220–231. https://pubmed.ncbi.nlm.nih.gov/29447449/ (Accessed June 20, 2022).
Hashimoto T, Wu Y, Boudreau N, Li J, Matsumoto M, Young W. 2004. Regulation of tie2 expression by angiopoietin--potential feedback system. *Endothelium* **11**: 207–210. https://www.ncbi.nlm.nih.gov/pubmed/15370298.
Hou X, Zaks T, Langer R, Dong Y. 2021. Lipid nanoparticles for mRNA delivery. *Nat Rev Mater* **6**: 1078–1094. https://www.ncbi.nlm.nih.gov/pubmed/34394960.
Kauffman KJ, Webber MJ, Anderson DG. 2016. Materials for non-viral intracellular delivery of messenger RNA therapeutics. *J Control Release* **240**: 227–234. https://www.ncbi.nlm.nih.gov/pubmed/26718856.
Keddissi JI, Youness HA, Jones KR, Kinasewitz GT. 2019. Fluid management in Acute Respiratory Distress Syndrome: A narrative review. *Canadian Journal of Respiratory Therapy: CJRT = Revue Canadienne de la Thérapie Respiratoire: RCTR* **55**: 1. /pmc/articles/PMC6591787/ (Accessed September 28, 2022).
Khan KA, Wu FT, Cruz-Munoz W, Kerbel RS. 2021. Ang2 inhibitors and Tie2 activators: potential therapeutics in perioperative treatment of early stage cancer. *EMBO Mol Med* **13**: e08253. https://www.ncbi.nlm.nih.gov/pubmed/34125494.
Kowalski PS, Rudra A, Miao L, Anderson DG. 2019. Delivering the Messenger: Advances in Technologies for Therapeutic mRNA Delivery. *Mol Ther* **27**: 710–728. https://www.ncbi.nlm.nih.gov/pubmed/30846391.
Leppänen VM, Saharinen P, Alitalo K. 2017. Structural basis of Tie2 activation and Tie2/Tie1

heterodimerization. *Proceedings of the National Academy of Sciences of the United States of America* **114**: 4376–4381. https://www.pnas.org/doi/abs/10.1073/pnas.1616166114 (Accessed October 10, 2022).

Matthay MA, Zemans RL, Zimmerman GA, Arabi YM, Beitler JR, Mercat A, Herridge M, Randolph AG, Calfee CS. 2019. Acute respiratory distress syndrome. *Nature Reviews Disease Primers 2019 5:1* **5**: 1–22. https://www.nature.com/articles/s41572-019-0069-0 (Accessed August 4, 2022).

McCarter SD, Mei SHJ, Lai PFH, Qiu WZ, Parker CH, Suen RS, Hood RD, Zhao YD, Deng Y, Han RNN, et al. 2007. Cell-based angiopoietin-1 gene therapy for acute lung injury. *American journal of respiratory and critical care medicine* **175**: 1014–1026. https://pubmed.ncbi.nlm.nih.gov/17322110/ (Accessed September 28, 2022).

Meyer NJ, Gattinoni L, Calfee CS. 2021. Acute respiratory distress syndrome. *The Lancet* **398**: 622–637. https://pubmed.ncbi.nlm.nih.gov/34217425/ (Accessed October 6, 2022).

Mitchell TJ, Walker JA, Saunders FK, Andrew PW, Boulnois GJ. 1989. Expression of the pneumolysin gene in Escherichia coli: rapid purification and biological properties. *Biochimica et biophysica acta* **1007**: 67–72. https://pubmed.ncbi.nlm.nih.gov/2642385/ (Accessed September 29, 2022).

Oh N, Kim K, Kim SJ, Park I, Lee JE, Seo YS, An HJ, Kim HM, Koh GY. 2015. A Designed Angiopoietin-1 Variant, Dimeric CMP-Ang1 Activates Tie2 and Stimulates Angiogenesis and Vascular Stabilization in N-glycan Dependent Manner. *Sci Rep* **5**: 15291. https://www.ncbi.nlm.nih.gov/pubmed/26478188.

Parikh SM, Mammoto T, Schultz A, Yuan HT, Christiani D, Karumanchi SA, Sukhatme VP. 2006. Excess circulating angiopoietin-2 may contribute to pulmonary vascular leak in sepsis in humans. *PLoS medicine* **3**: 356–370. https://pubmed.ncbi.nlm.nih.gov/16417407/ (Accessed September 28, 2022).

Saharinen P, Eklund L, Alitalo K. 2017a. Therapeutic targeting of the angiopoietin–TIE pathway. *Nature Reviews Drug Discovery 2017 16:9* **16**: 635–661. https://www.nature.com/articles/nrd.2016.278 (Accessed September 26, 2022).

Saharinen P, Leppanen VM, Alitalo K. 2017b. SnapShot: Angiopoietins and Their Functions. *Cell* **171**: 724-724 e1. https://www.ncbi.nlm.nih.gov/pubmed/29053972.

Santel A, Aleku M, Keil O, Endruschat J, Esche V, Durieux B, Loffler K, Fechtner M, Rohl T, Fisch G, et al. 2006a. RNA interference in the mouse vascular endothelium by systemic administration of siRNA-lipoplexes for cancer therapy. *Gene Ther* **13**: 1360–1370. https://www.ncbi.nlm.nih.gov/pubmed/16625242.

Santel A, Aleku M, Keil O, Endruschat J, Esche V, Fisch G, Dames S, Loffler K, Fechtner M, Arnold W, et al. 2006b. A novel siRNA-lipoplex technology for RNA interference in the mouse vascular endothelium. *Gene Ther* **13**: 1222–1234. https://www.ncbi.nlm.nih.gov/pubmed/16625243.

Seybold J, Thomas D, Witzenrath M, Boral Ş, Hocke AC, Bürger A, Hatzelmann A, Tenor H, Schudt C, Krüll M, et al. 2005. Tumor necrosis factor-α–dependent expression of phosphodiesterase 2: role in endothelial hyperpermeability. *Blood* **105**: 3569–3576. https://ashpublications.org/blood/article/105/9/3569/21288/Tumor-necrosis-factor-dependent-expression-of (Accessed September 29, 2022).

Srinivasan B, Kolli AR, Esch MB, Abaci HE, Shuler ML, Hickman JJ. 2015. TEER measurement techniques for in vitro barrier model systems. *Journal of laboratory automation* **20**: 107–126. https://pubmed.ncbi.nlm.nih.gov/25586998/ (Accessed September 28, 2022).

Tabruyn SP, Colton K, Morisada T, Fuxe J, Wiegand SJ, Thurston G, Coyle AJ, Connor J,

696 McDonald DM. 2010. Angiopoietin-2-Driven Vascular Remodeling in Airway
697 Inflammation. *The American Journal of Pathology* **177**: 3233.
698 /pmc/articles/PMC2993300/ (Accessed September 27, 2022).
699 Teder P, Vandivier RW, Jiang D, Liang J, Cohn L, Pure E, Henson PM, Noble PW. 2002.
700 Resolution of lung inflammation by CD44. *Science* **296**: 155–158.
701 https://www.ncbi.nlm.nih.gov/pubmed/11935029.
702 Thurston G, Rudge JS, Ioffe E, Zhou H, Ross L, Croll SD, Glazer N, Holash J, McDonald DM,
703 Yancopoulos GD. 2000. Angiopoietin-1 protects the adult vasculature against plasma
704 leakage. *Nature medicine* **6**: 460–463. https://pubmed.ncbi.nlm.nih.gov/10742156/
705 (Accessed September 27, 2022).
706 Thurston G, Suri C, Smith K, McClain J, Sato TN, Yancopoulos GD, McDonald DM. 1999.
707 Leakage-resistant blood vessels in mice transgenically overexpressing angiopoietin-1.
708 *Science (New York, NY)* **286**: 2511–2514. https://pubmed.ncbi.nlm.nih.gov/10617467/
709 (Accessed September 27, 2022).
710 Tiruppathi C, Malik AB, Del Vecchio PJ, Keese CR, Glaever I. 1992. Electrical method for
711 detection of endothelial cell shape change in real time: assessment of endothelial
712 barrier function. *Proceedings of the National Academy of Sciences of the United States*
713 *of America* **89**: 7919. /pmc/articles/PMC49826/?report=abstract (Accessed September
714 29, 2022).
715 Van Der Heijden M, Van Nieuw Amerongen GP, Koolwijk P, Van Hinsbergh VWM, Groeneveld
716 ABJ. 2008. Angiopoietin-2, permeability edema, occurrence and severity of ALI/ARDS in
717 septic and non-septic critically ill patients. *Thorax* **63**: 903–909.
718 https://pubmed.ncbi.nlm.nih.gov/18559364/ (Accessed September 27, 2022).
719 Villa E, Critelli R, Lasagni S, Melegari A, Curatolo A, Celsa C, Romagnoli D, Melegari G, Pivetti
720 A, Di Marco L, et al. 2021a. Dynamic angiopoietin-2 assessment predicts survival and
721 chronic course in hospitalized patients with COVID-19. *Blood Adv* **5**: 662–673.
722 https://www.ncbi.nlm.nih.gov/pubmed/33560382 (Accessed September 27, 2022).
723 Villa E, Critelli R, Lasagni S, Melegari A, Curatolo A, Celsa C, Romagnoli D, Melegari G, Pivetti
724 A, Di Marco L, et al. 2021b. Dynamic angiopoietin-2 assessment predicts survival and
725 chronic course in hospitalized patients with COVID-19. *Blood Adv* **5**: 662–673.
726 https://www.ncbi.nlm.nih.gov/pubmed/33560382.
727 Von Bethmann AN, Brasch F, Nüsing R, Vogt K, Volk HD, Müller KM, Wendel A, Uhlig S. 1998.
728 Hyperventilation induces release of cytokines from perfused mouse lung. *American*
729 *journal of respiratory and critical care medicine* **157**: 263–272.
730 https://pubmed.ncbi.nlm.nih.gov/9445308/ (Accessed September 29, 2022).
731 Wallace RG, Rochfort KD, Barabas P, Curtis TM, Uehara H, Ambati BK, Cummins PM. 2021.
732 COMP-Ang1: Therapeutic potential of an engineered Angiopoietin-1 variant. *Vascul*
733 *Pharmacol* **141**: 106919. https://www.ncbi.nlm.nih.gov/pubmed/34583025.
734 Wehrle C, Van Slyke P, Dumont DJ. 2009. Angiopoietin-1-induced ubiquitylation of Tie2 by c-
735 Cbl is required for internalization and degradation. *Biochem J* **423**: 375–380.
736 https://www.ncbi.nlm.nih.gov/pubmed/19689429.
737 Witzenrath M, Gutbier B, Hocke AC, Schmeck B, Hippenstiel S, Berger K, Mitchell TJ, De Los
738 Toyos JR, Rosseau S, Suttorp N, et al. 2006. Role of pneumolysin for the development of
739 acute lung injury in pneumococcal pneumonia. *Critical Care Medicine* **34**: 1947–1954.
740 Wu FT, Lee CR, Bogdanovic E, Prodeus A, Gariépy J, Kerbel RS. 2015. Vasculotide reduces
741 endothelial permeability and tumor cell extravasation in the absence of binding to or
742 agonistic activation of Tie2. *EMBO molecular medicine* **7**: 770–787.
743 https://pubmed.ncbi.nlm.nih.gov/25851538/ (Accessed September 29, 2022).

744 **Figure 1**

745

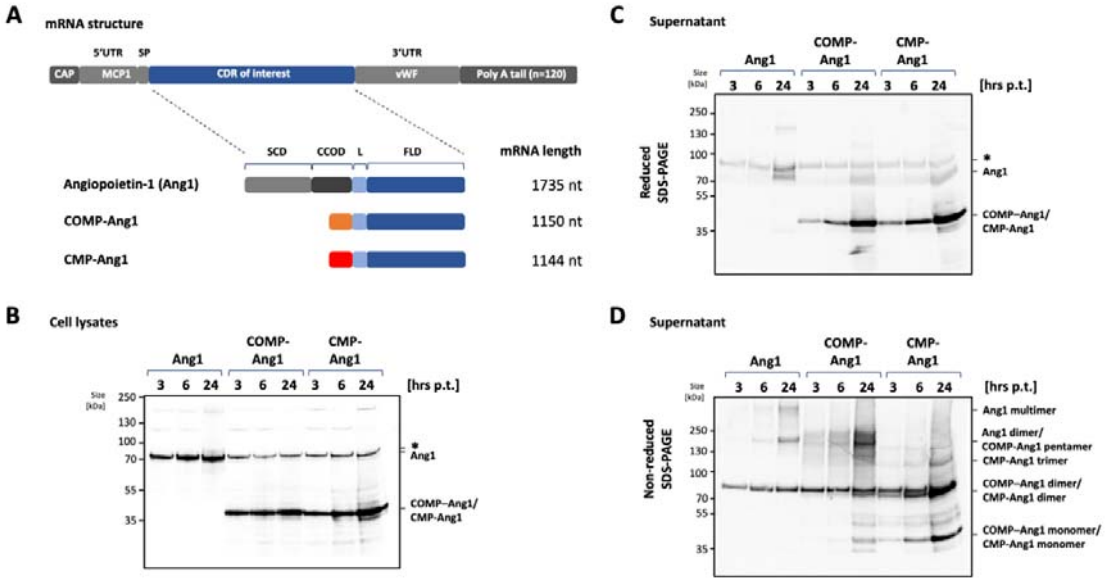

746
747
748

749 **Figure 1: mRNA directed expression, secretion and multimerization of human Ang1,**

750 **COMP-Ang-1 and CMP-Ang1 *in vitro*.**

751 **(A)** General structure of mRNA with signal peptide (SP) sequence flanked by designated 5´-
752 and 3´- UTR regions plus defined polyA-tail. Schematic representation of protein domain
753 structure of the natural protein Ang1 and the derived engineered humanized fusion proteins
754 COMP-Ang1 and CMP-Ang1 according to Cho et al.,2004 and Oh et al., 2015. Protein
755 domains of human Ang1: SCD, super clustering domain; CCOD, coiled coil domain; L, linker;
756 FLD, Fibrinogen-related domain; the multimerization domains of COMP (orange) and of CMP
757 protein (red) are indicated. **(B)** Expression, **(C)** secretion and **(D)** multimerization of wt Ang1
758 and Ang1 derivates in Hela cells. Cells were transfected for 2 h with mRNA-52 encoding
759 Ang1, mRNA-76 encoding COMP-Ang1, or mRNA-59 encoding CMP-Ang1. Cell lysates and
760 supernatants were harvested at indicated time points post transfection (p.t.) and analyzed
761 by Western blotting using Ang1-specific antibody. (*, unidentified band)

762

763 **Figure 2**

764

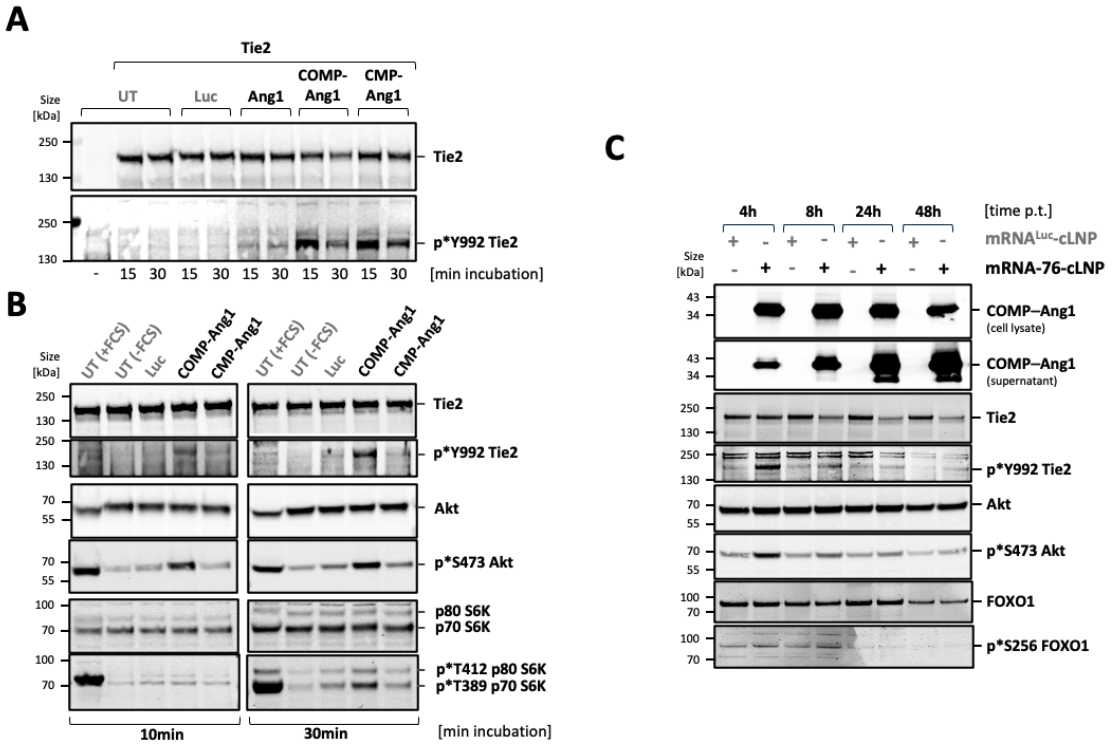

765

766

767

768 **Figure 2: Activation of Tie2 pathway by Ang1, COMP-Ang1 and CMP-Ang1 containing**

769 **supernatants**

770 **(A)** Immunoblot of Tie2 expression and Tie2 phosphorylation from Tie2-expressing Hela cells
771 after 15 or 30 min incubation with supernatant from HeLa cells expressing Luc, Ang1, COMP-
772 Ang1 and CMP-Ang-1 (see Fig. 1) following incubation with supernatants from Hela cells
773 transfected for 24h with Luc-mRNA or mRNA-52 encoding Ang1, mRNA-76 encoding COMP-
774 Ang1, and mRNA-59 encoding CMP-Ang1. **(B)** Activation of Tie2 pathway in serum-starved
775 primary human pulmonary microvascular endothelial cells (HPMEC) by COMP-Ang1 and by
776 CMP-Ang1 containing supernatant from mRNA-76 or mRNA-59 transfected HeLa cells. Tie2-
777 pathway activation is demonstrated by analysis of Tie2 phosphorylation status and by
778 presence of phosphorylation at the downstream effectors Akt and S6K. **(C)** Tie2-pathway
779 activation after transfection of LNP-formulated, COMP-Ang1-encoding mRNA-76 in serum-
780 starved HPMEC. COMP-Ang1 expression, secretion, Tie2, Akt, and FOXO1 phosphorylation is
781 shown by immunoblot on cell lysates at different time points post transfection (p.t.). (UT,
782 untreated; FCS, Fetal calf serum; Luc, control Nano-Luciferase-encoding mRNA).

783

784 **Figure 3**

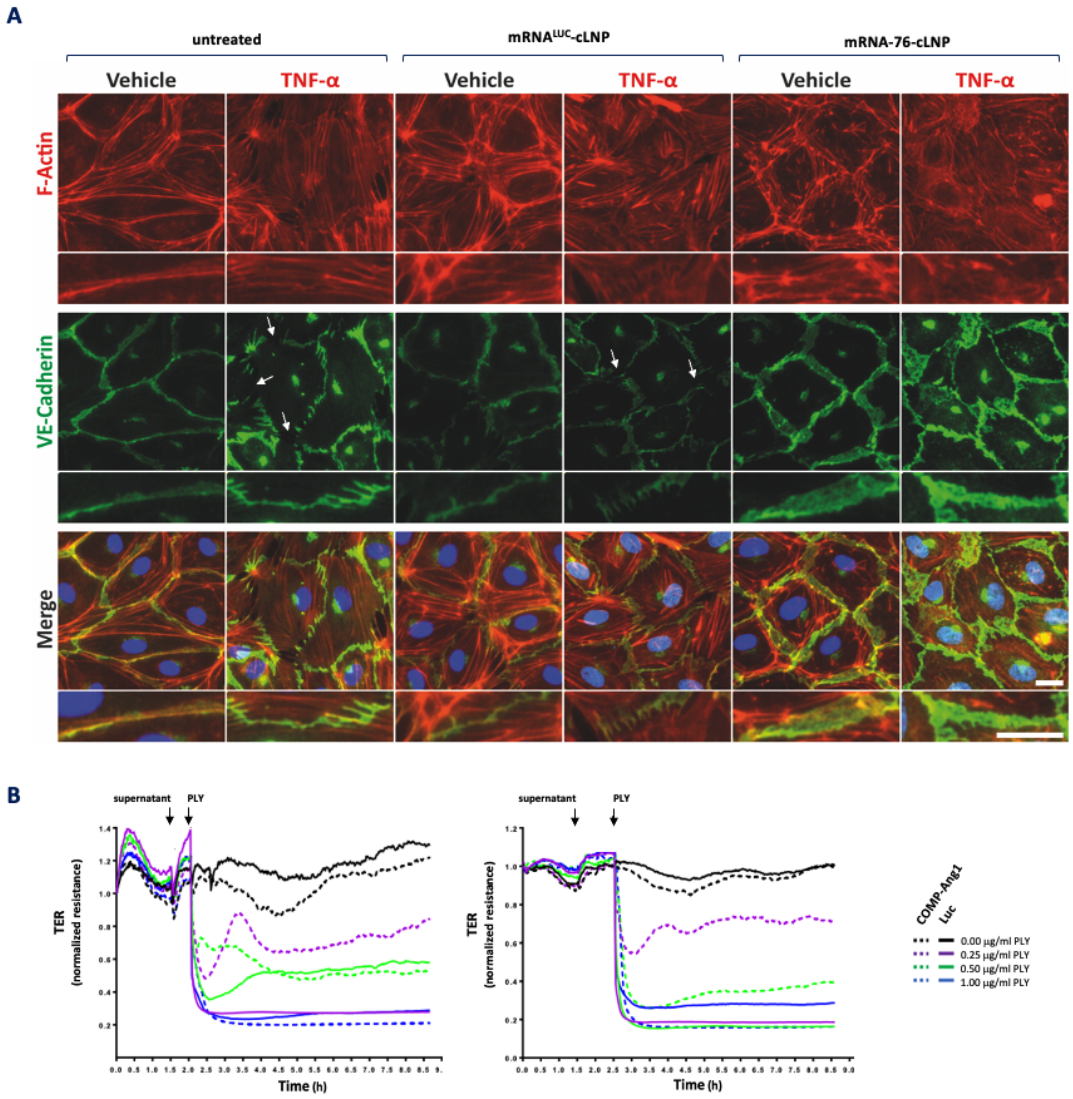

785

786

787 **Figure 3: Cell staining by immunofluorescence demonstrating stabilization of endothelial**

788 **adherens junctions.**

789 **(A)** Effect of COMP-Ang1 on F-actin remodeling and VE-Cadherin distribution in isolated

790 human pulmonary microvascular endothelial cell. HPMECs grown on glass coverslips were

791 transfected for 24h with control mRNA^{LUC} or with mRNA-76 encoding COMP-Ang1 with or

792 without temporal addition of 10 ng/ml TNFα, followed by immunofluorescence staining with

793 VE-Cadherin-specific antibody and with Alexa Fluor 594 phalloidin to detect actin filaments.

794 Arrows indicate disrupted VE-Cadherin complexes. **B)** Transcellular electrical resistance (TER)

795 measurements of HPMEC monolayers. HPMEC were incubated for 30 min (top) or 60 min

(bottom) with supernatant from mRNA-76 or with $mRNA^{LUC}$ (Luciferase) and the treated with supernatants from Hela cells transfected for 24 h with control $mRNA^{LUC}$ or mRNA-76 encoding COMP-Ang1 and stimulated with indicated amount of pneumolysin (PLY; 0.25, 0.5, 0.75, 1.0 µg/ml). PLY stimulation decreased TER of HPMEC monolayers, displaying loss of endothelial integrity when incubated with control Luciferase supernatant (solid curve). Preincubation with COMP-Ang1 containing supernatant attenuated the PLY-induced TER decrease (purple lines dashed versus solid).

827 **Figure 4**

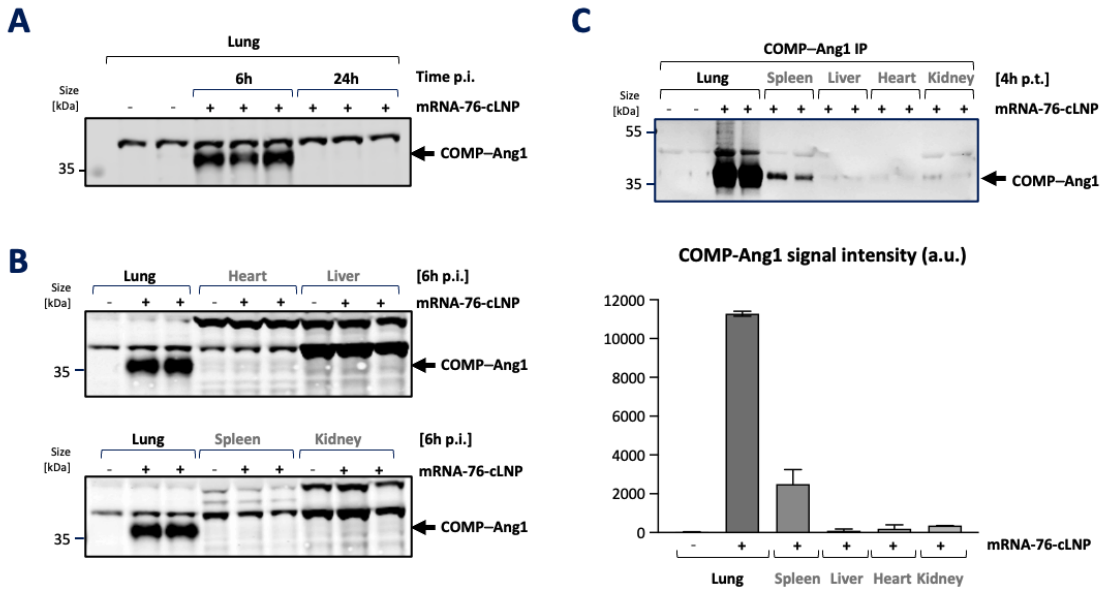

828

829 **Figure 4. Transient expression of COMP-Ang1 in murine lungs by cLNP-mediated lung**
830 **delivery of mRNA-76**

831 **(A)** Immunoblot of lung tissue lysates 6 and 24 h after administration of 1.5 mg/kg mRNA-76-
832 cLNP (+) or saline control (-). The expressed COMP-Ang1 fusion protein is indicated by an
833 arrow. **(B)** Immunoblot of different tissue lysates 6h post-administration of 1.5 mg/kg mRNA-
834 76-cLNP (+) or saline control (-). Lung selective COMP-Ang1 protein is indicated by an arrow.
835 **(C)** Immunoprecipitation of COMP-Ang1 protein using Tie2-Fc-coupled magnetic beads from
836 indicated tissue samples 4 h after administration of 1.5 mg mRNA-76-cLNP (+) or saline
837 control (-).

838

839

840

841

842

843 **Figure 5**

844

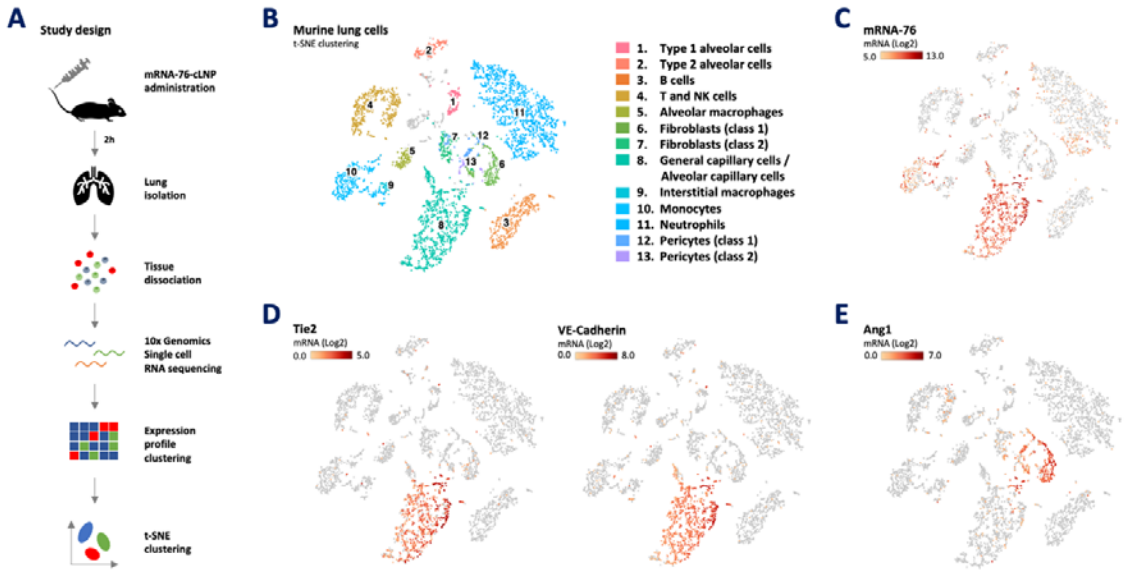

845

846

847 **Figure 5: cLNP-mediated delivery of 1.5 mg/kg mRNA-76 leads to uptake predominantly in**
848 **murine pulmonary capillary endothelial cells.**

849 **(A)** Experimental design and workflow (**B**) Loupe-based t-distributed stochastic neighbor
850 embedding (t-SNE) clustering of murine lung cell types clustered by single-cell transcriptional
851 analysis of 5,100 cells after quality control, showing a total of 13 distinct cell type clusters as
852 indicated by numbers. **(C)** t-SNE plots showing levels for COMP-Ang1-encoding mRNA-76. **(D)**
853 t-SNE plots showing levels for canonical markers of endothelial cells (Tie2, VE-Cadherin). **(F)**
854 cells expressing Ang1 (pericytes class 1 and 2, fibroblasts class 1). The intensity of expression
855 is indicated by red coloring.

856

857

858

859

860

861

862

863 **Figure 6**

864

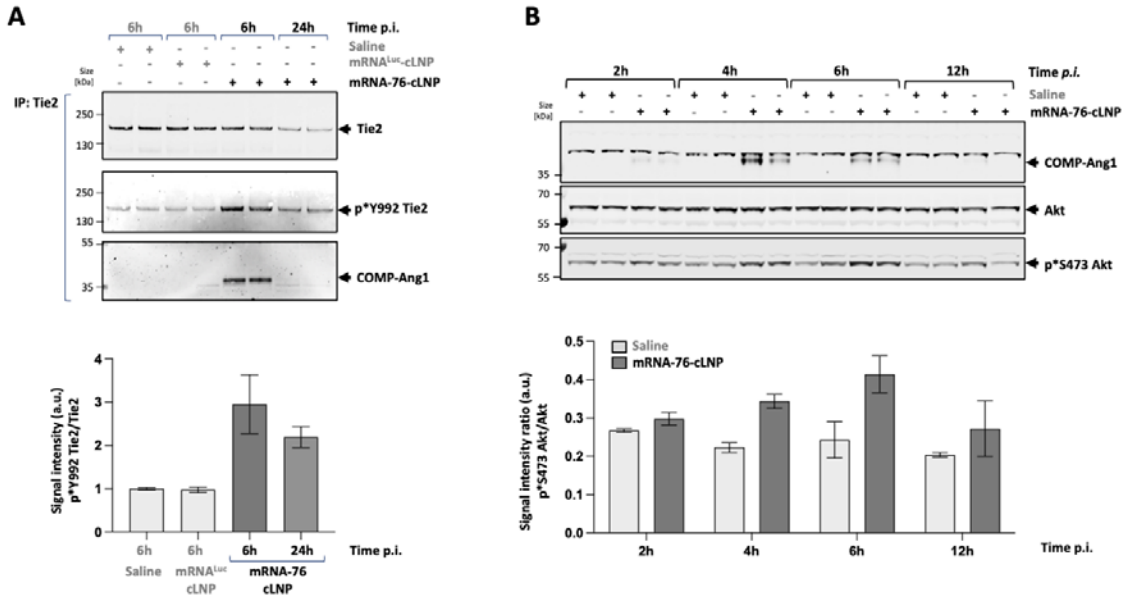

865

866

867 **Figure 6: cLNP-mediated delivery of mRNA-76 leads to time-dependent Tie2 pathway**
868 **activation *in vivo*.**

869 **(A)** Immunoblot after immunoprecipitation of murine Tie2 from lung samples at indicated
870 time points after i.v. administration of 1.5 mg/kg mRNA-76-cLNP. **(B)** Immunoblot of murine
871 lunge tissue lysates analyzing COMP-Ang1 expression level and Akt phosphorylation status at
872 indicated time points after i.v. administration of 1.5 mg/kg mRNA-76-cLNP or Saline.

873

874

875

876

877

878

879

880

881

882

883

884

885 **Figure 7**

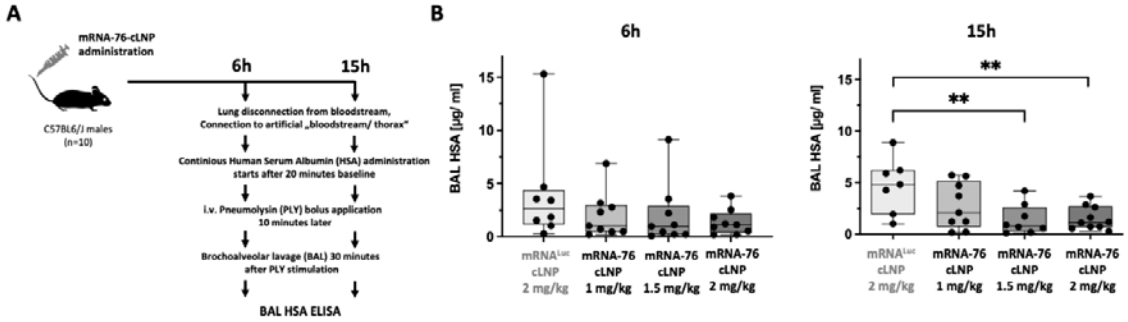

886

887

888 **Figure 7: Systemic mRNA-76 treatment stabilized endothelial barrier lung function in an *ex***
889 ***vivo* isolated perfused and ventilated mouse lung (IPML) model.**

890 **(A)** Schematic diagram of the experimental protocol of the *ex vivo* perfused and ventilated
891 mouse lung model. 6 h, 15 h after administration of mRNA-76-cLNP (1, 1.5 and 2 mg/kg) or
892 control $mRNA^{LUC}$-LNP (2 mg/kg) lungs were isolated and stimulated with PLY (1.4 µg/ml) for 1
893 minute. After 30 min, lung vascular permeability was assessed by quantifying respective
894 concentrations of continuously infused human serum albumin (HSA) in the bronchoalveolar
895 lavage fluid (BALF). **(B)** Graphic showing treatment with mRNA-76 to significantly decrease
896 pneumolysin-induced hyperpermeability of mouse lungs as compared to treatment with
897 control $mRNA^{LUC}$-LNP 6 h (left) and 15 h (right) post mRNA-76-cLNP treatment as shown by
898 HAS ELISA. Values are given as mean (n=10, **$p<0.01$ between indicated groups)
899 concentration of human serum albumin (HSA) in bronchoalveolar lavage fluid (BALF). HSA
900 concentration of individual mice are indicated as dots.

901

902

903

904

905

906

907

908

909

910

911 **Figure 8**

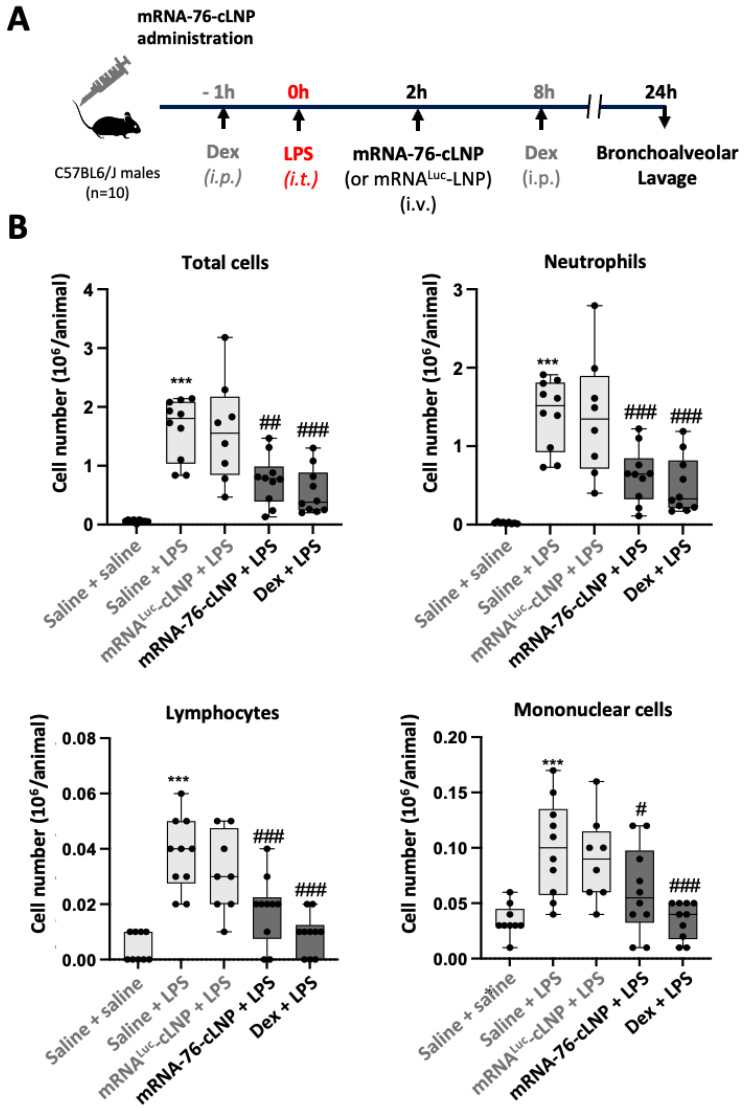

912

913

914 **Figure 8**: **LPS-induced Pulmonary Neutrophilia Mouse Model**

915 **(A)** Schematic drawing of the experimental protocol. Animals (n=10) were challenged
916 intratracheally with 0.9% w/v saline or LPS (3 mg/kg). A fixed volume of 50 µL, equal to an
917 approximate intratracheal dose volume of 2.5 mL/kg, based on a 20 g mouse, was applied
918 intratracheally. 2h after LPS administration mRNA-76-cLNP (1.5 mg/kg IV) or mRNA^{LUC}-
919 cLNP01 (1.5 mg/kg IV) was intravenously administered, and bronchoalveolar lavage fluid
920 (BALF) was analysed after 24 h. **(B)** Effect of COMP-Ang1 expression on BALF total and
921 differential cell counts and on wet lung weight in a murine model of endotoxin (LPS)-induced
922 pulmonary inflammation. Data shown as mean ± standard error of the

923 mean. *** $p<0.001$ when compared to saline challenged control group. # $p<0.05$, ## $p<0.01$,

924 ### $p<0.001$ as compared to LPS challenged and vehicle treated group.

925

926
927
928
929
930
931
932
933
934
935
936

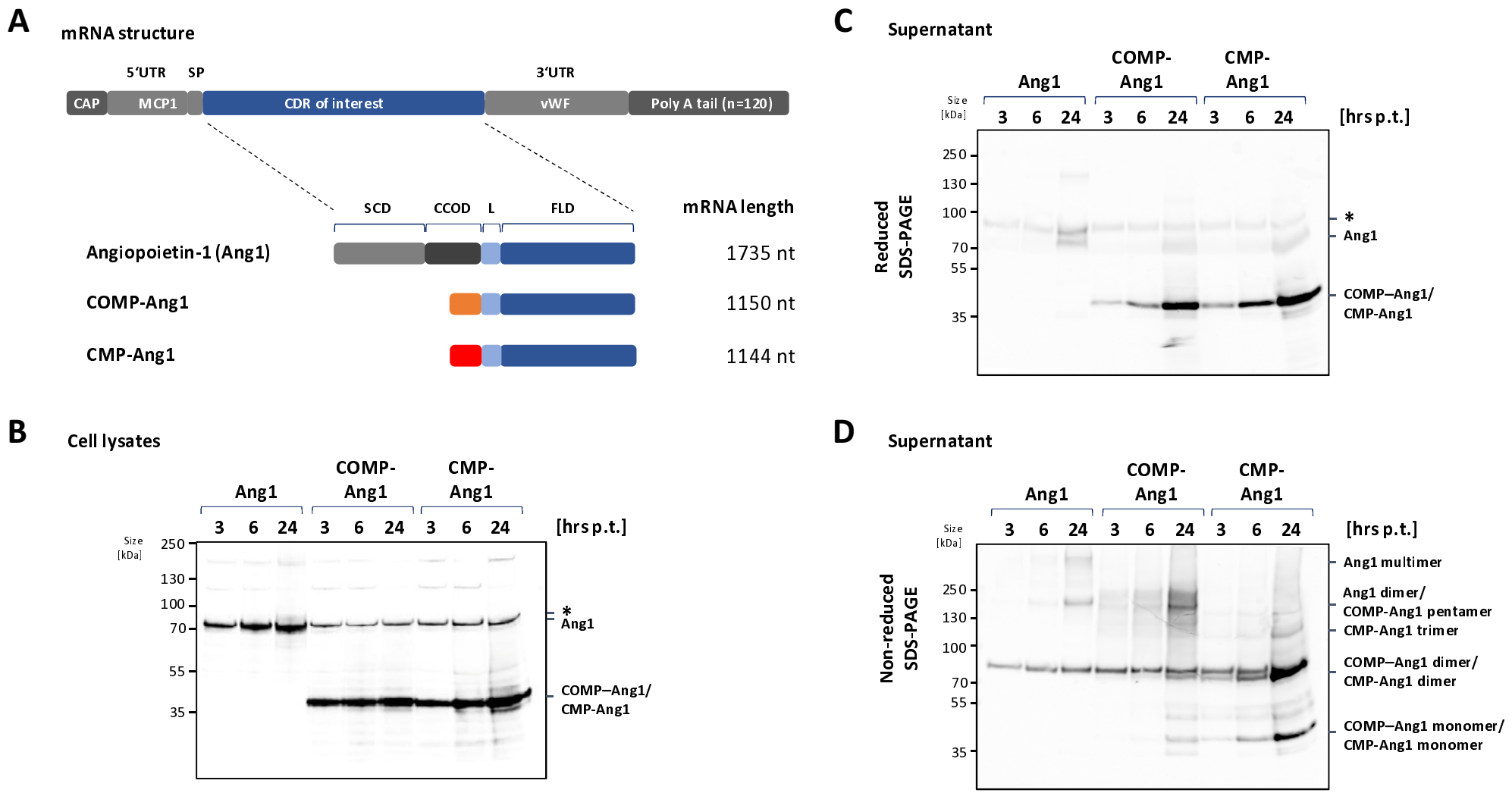

ected expression, secretion and multimerization of human Ang1, COMP-Ang-1 and CMP-Ang1 in vitro

re of mRNA with signal peptide (SP) sequence flanked by designated 5´- and 3´- UTR regions plus defined polyA-tail. Schematic representation of protein domain structure of the natural prot
d humanized fusion proteins COMP-Ang-1 and CMP-Ang1 according to Cho et al.,2004 and Oh et al., 2015. Protein domains of human Ang1: SCD, super clustering domain; CCOD, coiled coil do
ated domain; the multimerization domains of COMP (orange) and of CMP protein (red) are indicated. (**B**) Expression, (**C**) secretion and (**D**) multimerization of wt Ang1 and Ang1 derivates in H
or 2h with mRNAs encoding for indicated Ang1 variants. Cell lysates and supernatants were harvested at indicated time points post transfection (p.t.) and analyzed by Western blotting using A
ntified band)

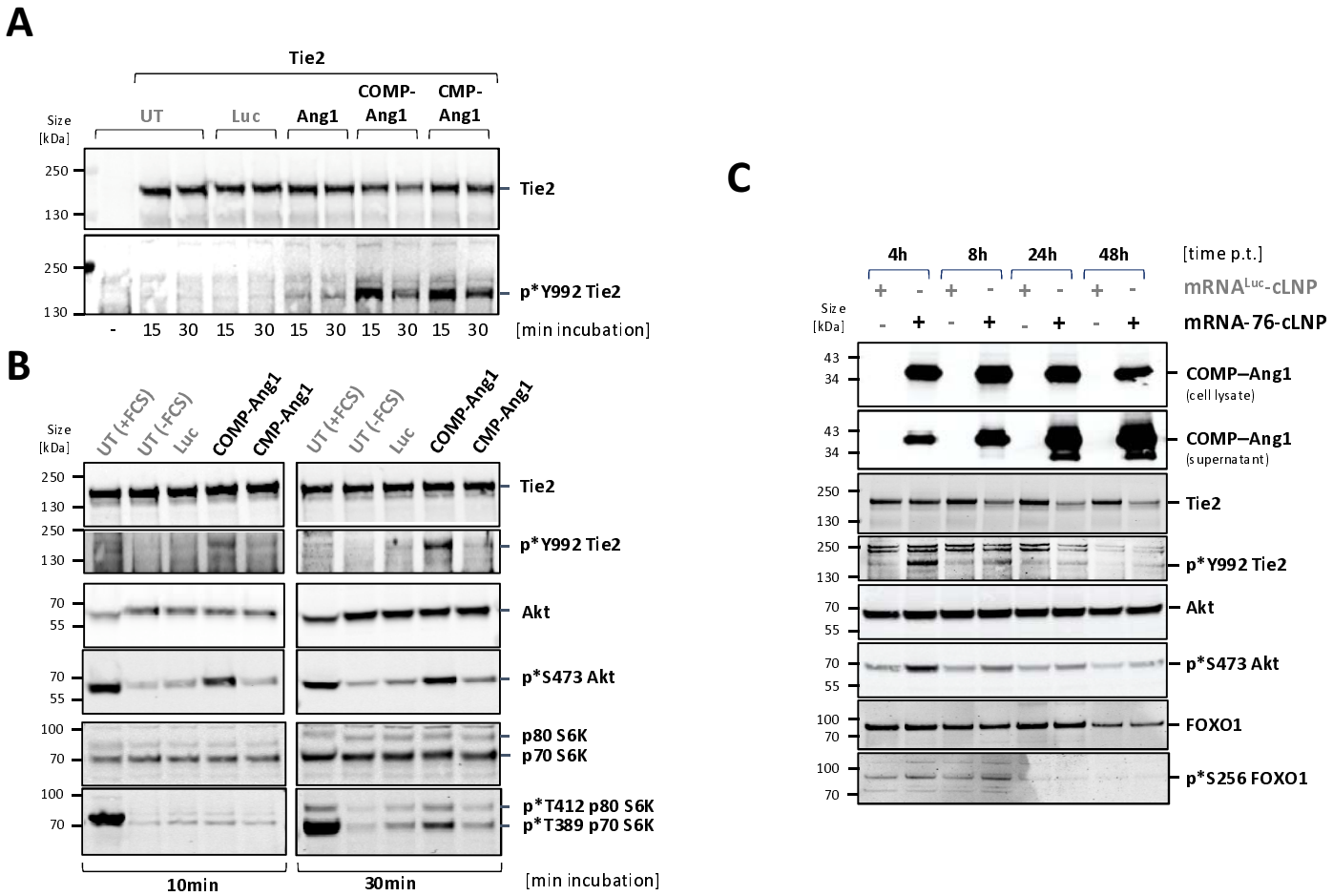

of Tie2 pathway by Ang-1, COMP-Ang1 and CMP-Ang1 containing supernatants

e2 expression and Tie2 phosphorylation from Tie2-expressing Hela cells after 15 or 30 min incubation with supernatant from HeLa cells expressing Luc, Ang-1, COMP-Ang1 and CMP-Ang-1 (se with supernatants from Hela cells transfected for 24h with Luc-mRNA or mRNA-52 encoding Ang1, mRNA-76 encoding COMP-Ang1, and mRNA-59 encoding CMP-Ang1 **(B)** Activation of Tie2 p ry human pulmonary microvascular endothelial cells (HPMEC) by COMP-Ang1 and by CMP-Ang-1 containing supernatant from mRNA-76 or mRNA-59 transfected HeLa cells. Tie2-pathway acti ılyzing Tie2 phosphorylation status and by presence of phosphorylation at the downstream effectors Akt and S6K. **(C)** Tie2-pathway activation after transfection of LNP-formulated COMP-Ang: :arved HPMEC. COMP-Ang-1 expression, secretion, Tie2, Akt, and FOXO1 phosphorylation is shown by immunoblot on cell lysates at different time points post transfection (p.t.). (UT, untreate ano-Luciferase-encoding mRNA)

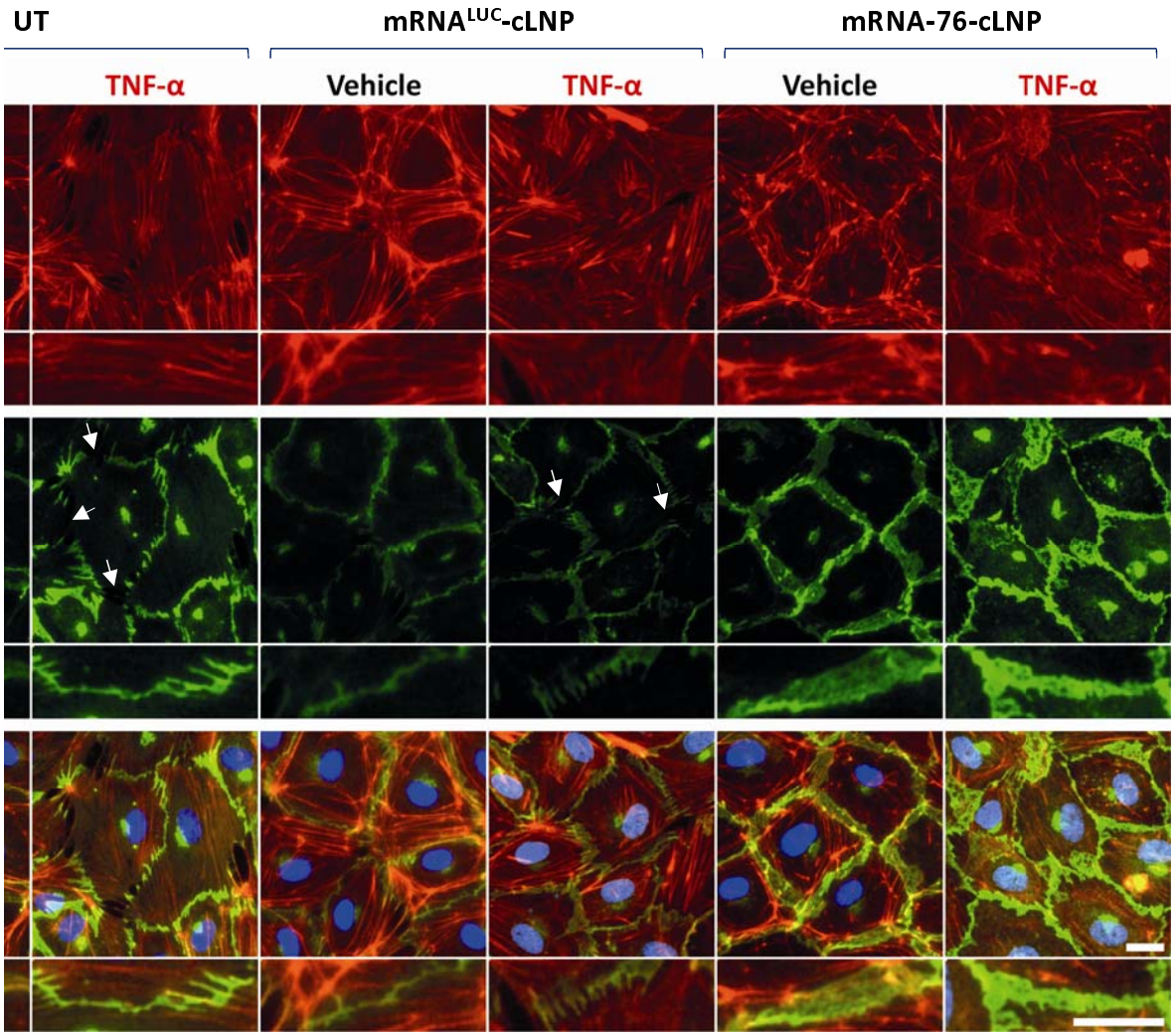

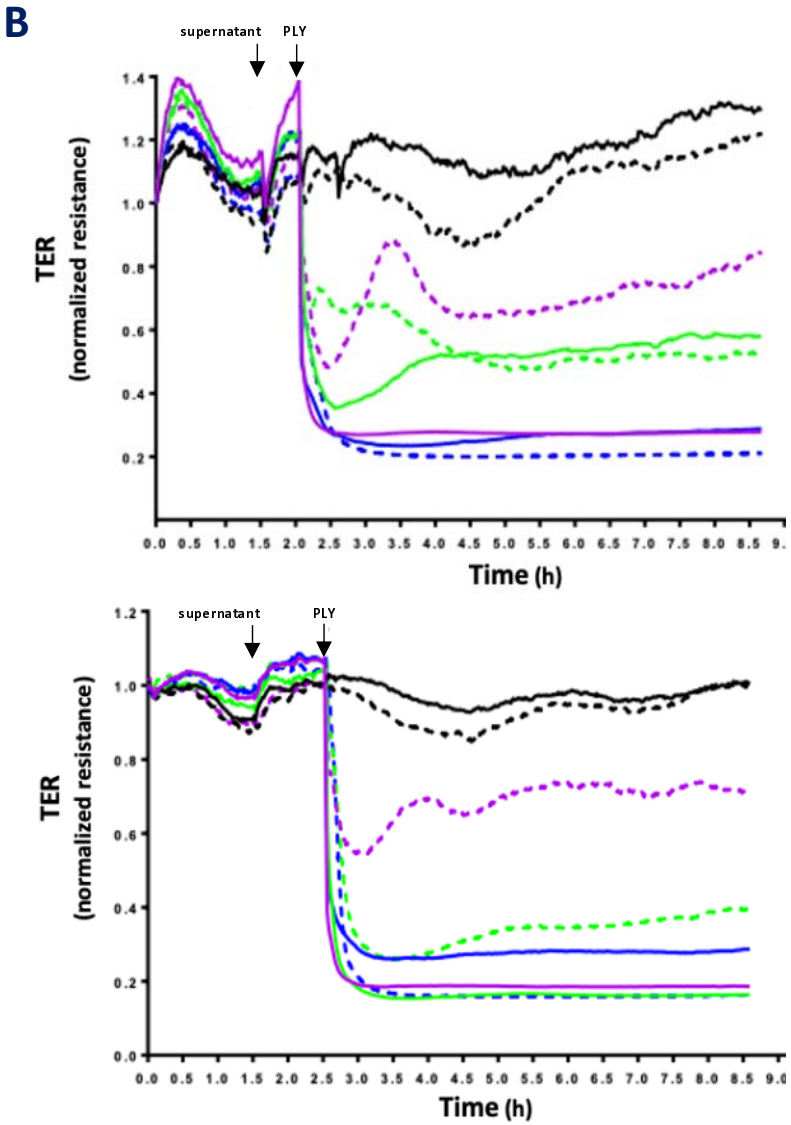

ing by immunofluorescence demonstrating stabilization of endothelial adherens junctions. **A)** Effect of COMP-Ang1 on F-actin remodeling and VE-Cadherin distribution in isolated human pu
ɔthelial cell. HPMECs grown on glass coverslips were transfected for 24h with control mRNA^{LUC} or with mRNA-76 encoding COMP-Ang1 with or without temporal addition of 10ng/ml TNFα, fol
ce staining with VE-Cadherin-specific antibody and with Alexa Fluor 594 phalloidin to detect actin filaments. Arrows indicate disrupted VE-Cadherin complexes. **B)** Transcellular electrical resist
HPMEC monolayers. HPMEC were incubated for 30 min (top) or 60 min (bottom) with supernatant from mRNA-76 or with mRNA^{Luc} (Luciferase) and the treated with supernatants from Hela ce
ɔl mRNA^{LUC} or mRNA-76 encoding COMP-Ang1 and stimulated with indicated amount of pneumolysin (PLY; 0.25, 0.5, 0.75, 1.0 µg/ml). PLY stimulation decreased TER of HPMEC monolayers, di
:y when incubated with control Luciferase supernatant (solid curve). Preincubation with COMP-Ang1 containing supernatant attenuated the PLY-induced TER decrease (purple lines dashed ve

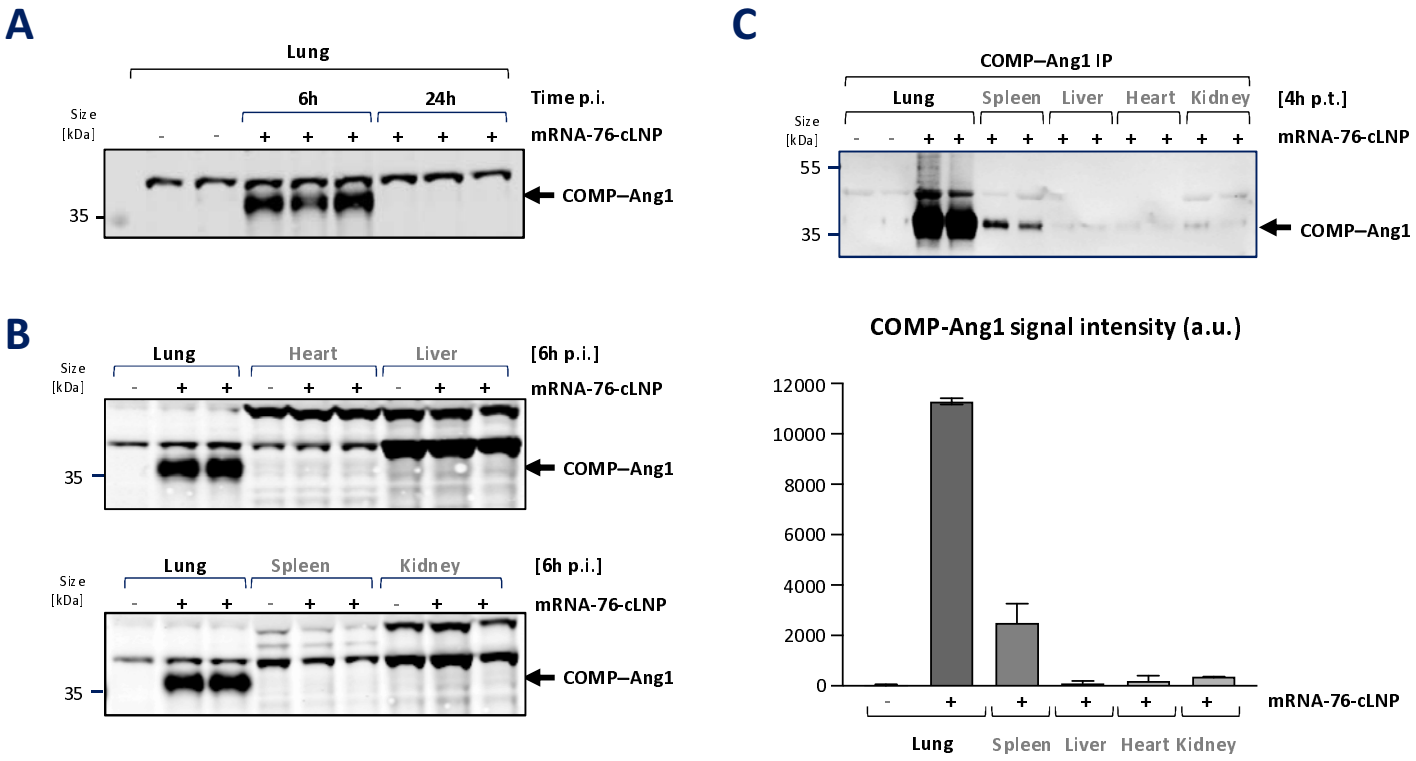

nt expression of COMP-Ang1 in murine lungs by cLNP-mediated lung delivery of mRNA-76
of lung tissue lysates 6 and 24h after administration of 1.5 mg/kg mRNA-76-cLNP (+) or saline control (-). The expressed COMP-Ang1 fusion protein is indicated by an arrow.
of different tissue lysates 6h after post-administration of 1.5 mg/kg mRNA-76-cLNP (+) or saline control (-). Lung selective COMP-Ang-1 protein is indicated by an arrow.
pitation of COMP-Ang1 using Tie2-Fc from indicated tissue samples 4h after administration of 1.5mg mRNA-76-cLNP (+) or saline control (-).

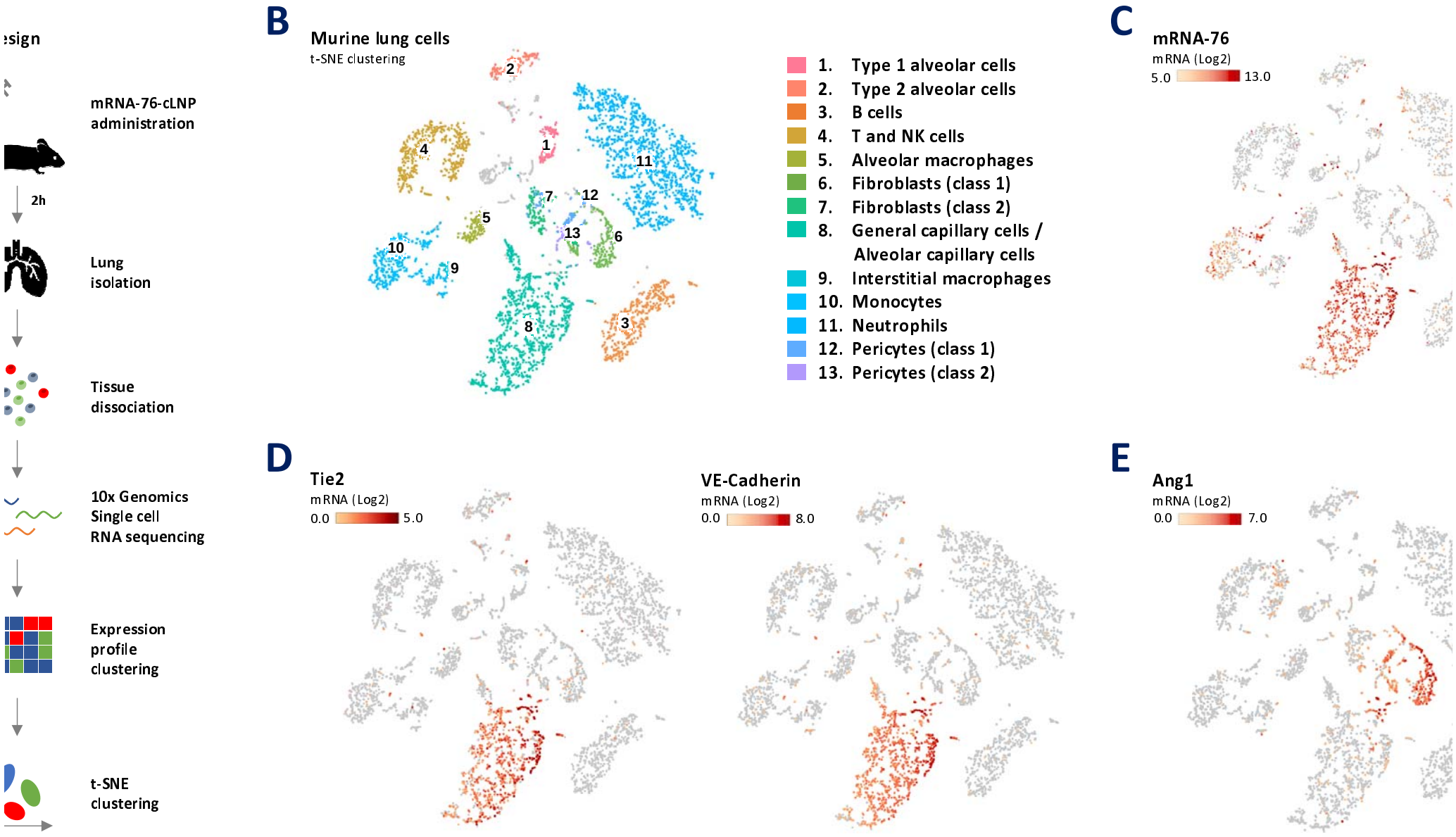

diated delivery of 1.5 mg/kg mRNA-76 leads to uptake predominantly in murine pulmonary capillary endothelial cells. **(A)** Experimental design and workflow (**B**) Loupe-based t-distributed s
l clustering of murine lung cell types clustered by single-cell transcriptional analysis of 5,100 cells after quality control, showing a total of 13 distinct cell type clusters as indicated by numb
COMP-Ang1-encoding mRNA-76. **(D)** t-SNE plots showing levels for canonical markers of endothelial cells (Tie2, VE-Cadherin). **(F)** cells expressing Ang1 (pericytes class 1 and 2, fibroblasts cla
licated by red coloring.

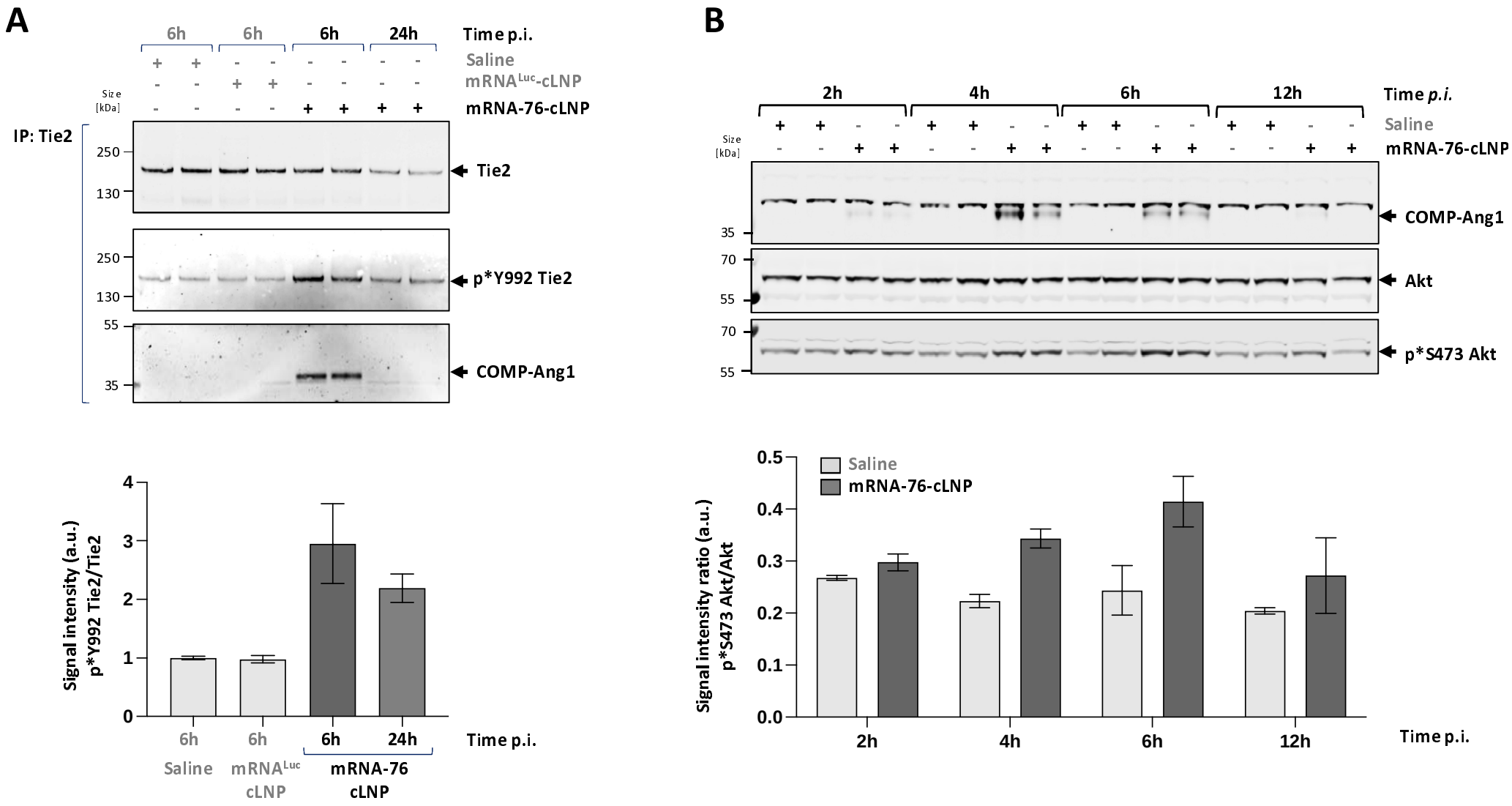

diated delivery of mRNA-76 leads to time-dependent Tie2 pathway activation in vivo

:er immunoprecipitation of murine Tie2 from lung samples at indicated time points after i.v. administration of 1.5 mg/kg mRNA-76-cLNP. (B) Immunoblot of murine lunge tissue lysates analys

vel and Akt phosporylation status at indicated time points after i.v. administration of 1.5 mg/kg mRNA-76-cLNP or Saline.

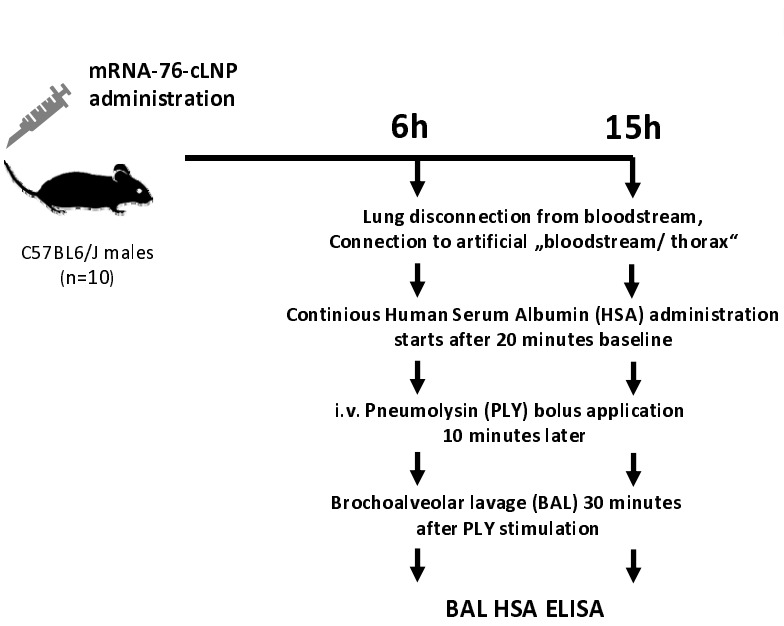

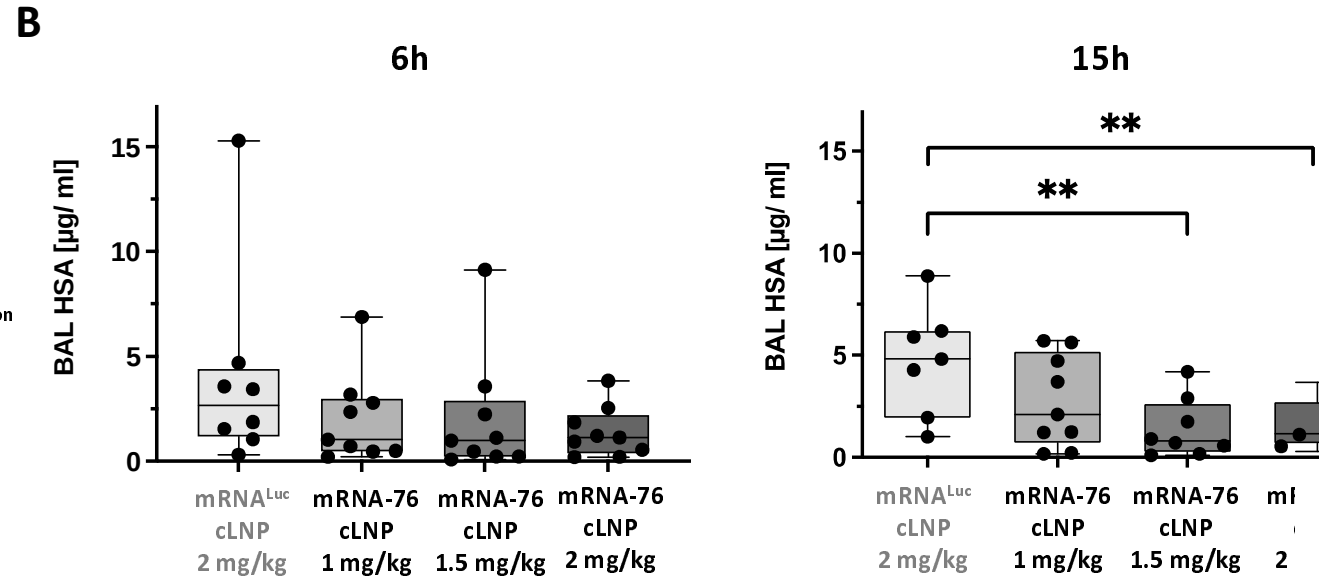

mRNA-76 treatment stabilized endothelial barrier lung function in an *ex vivo* isolated perfused and ventilated mouse lung (IPML) model (A) Schematic diagram of the experimental protoc
ventilated mouse lung model. 6 h, 15 h after administration of mRNA-76-cLNP (1, 1.5 and 2 mg/kg) or control mRNA^{LUC}-LNP (2 mg/kg) lungs were isolated and stimulated with PLY (1.4 µg/ml) f
vascular permeability was assessed by quantifying respective concentrations of continuously infused human serum albumin (HSA) in the bronchoalveolar lavage fluid (BALF). **(B)** Graphic showi
gnificantly decrease pneumolysin-induced hyperpermeability of mouse lungs as compared to treatment with control mRNA^{LUC}-LNP 6 h (left) and 15 h (right) post mRNA-76-cLNP treatment as
ven as mean (n = 10, **p<0.01 between indicated groups) concentration of human serum albumin (HSA) in bronchoalveolar lavage fluid (BALF). HSA concentration of individual mice are indica

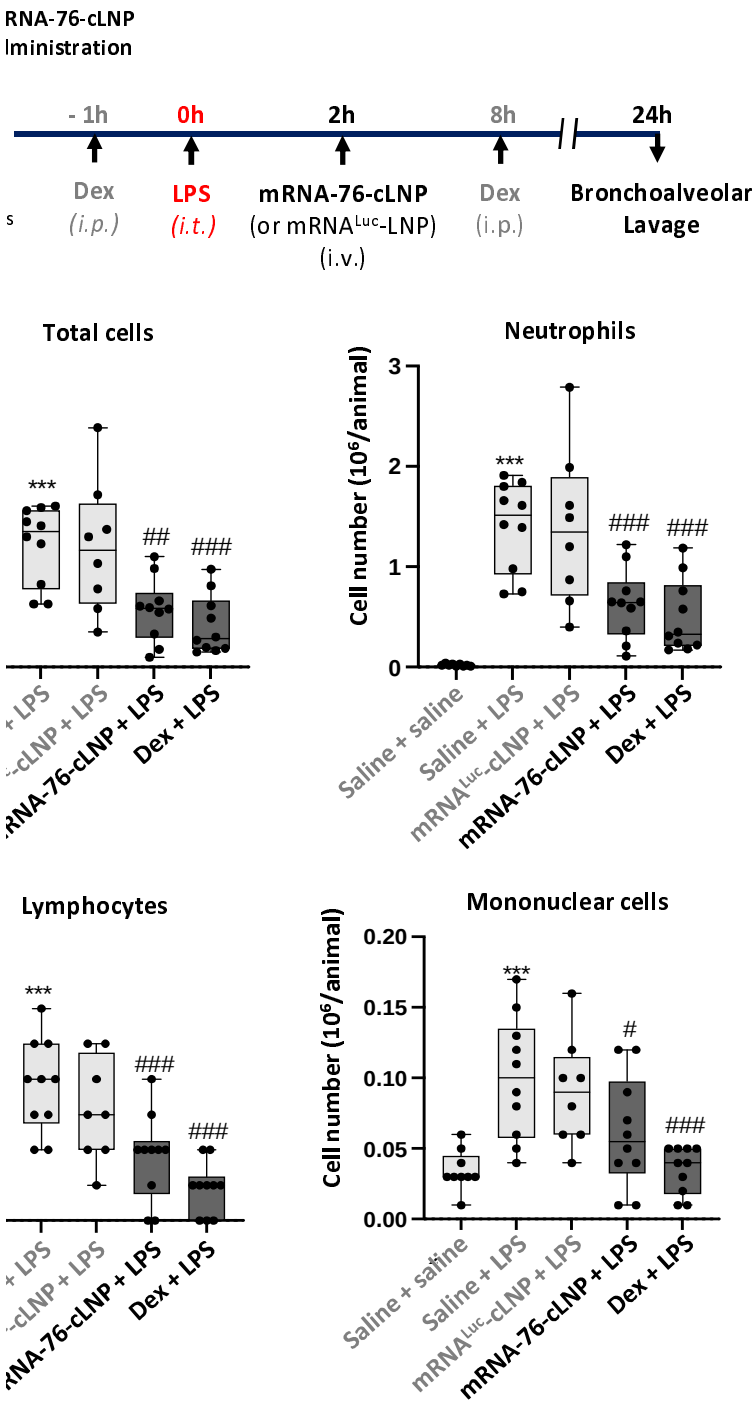

Figure 8: **LPS-induced Pulmonary Neutrophilia Mouse Model (A**) Schematic drawing of the experimenta
Animals (n=10) were challenged intratracheally with 0.9% w/v saline or LPS (3 mg/kg). A fixed volume of 5
an approximate intratracheal dose volume of 2.5 mL/kg, based on a 20 g mouse, was applied intratrachea
LPS administration mRNA-76-cLNP (1.5 mg/kg IV) or mRNA^{LUC}-cLNP01 (1.5 mg/kg IV) was intravenously ad
and bronchoalveolar lavage fluid (BAL) was analysed after 24 h. **(B)** Effect of COMP-Ang1 expression on BA
differential cell counts and on wet lung weight in a murine model of endotoxin (LPS)-induced pulmonary i
Data shown as mean ± standard error of the mean. *** p<0.001 when compared to saline challenged cor
group. # p<0.05, ## p<0.01, ### p<0.001 as compared to LPS challenged/vehicle treated group.